同濟大學 TONGJI UNIVERSITY

Effects of Shot Peening on Fatigue Crack Initiation and Propagation Performance

Yukui GAO
Tongji University
Email: yukuigao@tongji.edu.cn

Outline

1 Introduction

2 Experimental

2.1 Fatigue strength/limits of smooth fatigue specimens-fatigue damage/cracking

2.2 Small crack propagation and fatigue life in residual stress fields-crack growth

3 Results and discussion

3.1 Fatigue crack initiation and fatigue strength/limits

3.2 Fatigue crack propagation and fatigue life prediction

4 Conclusions and recommendations

1 Introduction

What is surface integrity? Its Effects?

Surface Integrity is the inherent or enhanced condition of a surface produced in a machining or other surface generation operation.

Surface Condition and Performance/Property

1. retard fatigue crack initiation and propagation
2. improve fatigue, fretting fatigue, corrosion fatigue, stress corrosion cracking, pit corrosion and wear resistance

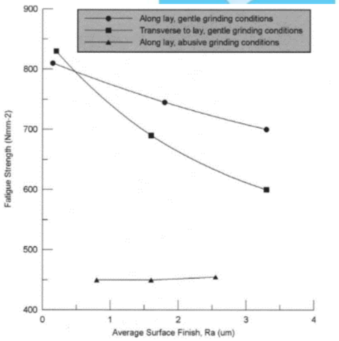

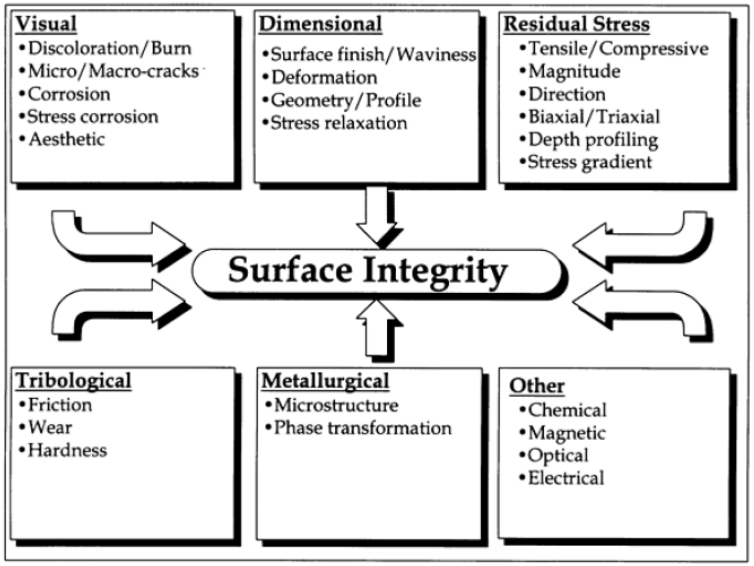

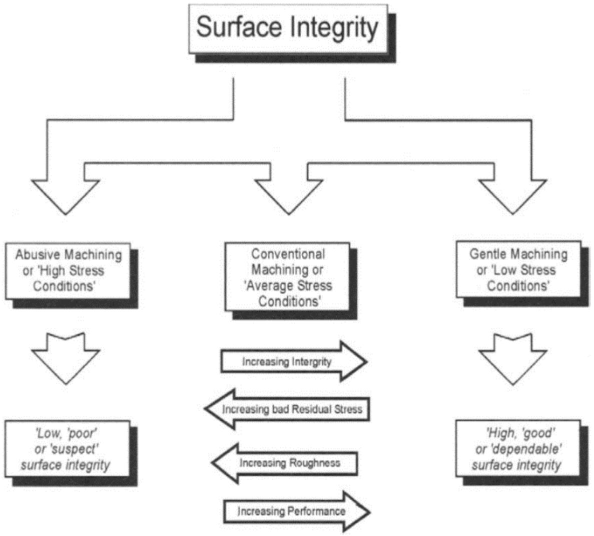

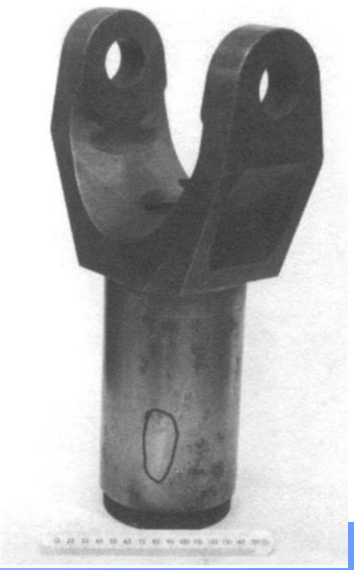

Many high strength or ultrahigh strength metallic materials are used. For these metallic alloys, the fatigue properties are affected mainly by surface treatments. To improve the fatigue properties, surface enhancement processes are applied to modify the surface integrity.

In the views of fatigue property, the main parameters of surface integrity are residual stresses in surface layer, surface roughness and microstructure. The structural integrity is mainly determined by surface integrity because many fractures occur at surfaces, especially at some defects.

It is necessary and important to quantitatively determine the effects of surface enhancements for designing components with surface-enhanced layers.

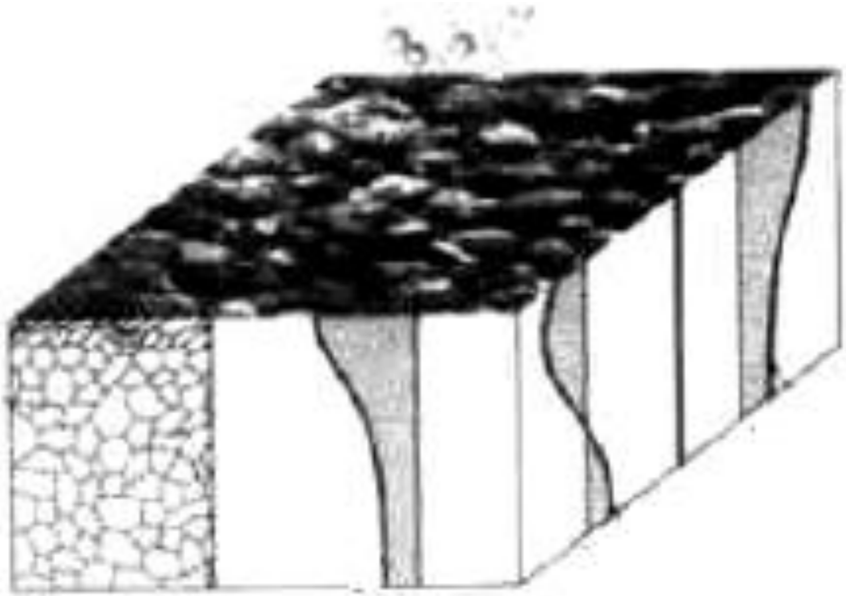

Objectives

Provide a method to quantitatively evaluate the effect of shot peening on fatigue strength

Present some methods to predict crack propagation life in residual stress fields

Propose new models to analyze the effects of surface integrity on fatigue life

Give some means to define fatigue strength enhancement limited percentage and how to evaluate the optimal process parameters

2 Experimental

2.1 Fatigue strength or fatigue limits of shot-peened smooth fatigue specimens

High or ultrahigh strength steels, aluminum alloys and titanium alloys were used and their tensile properties are listed in Table 1.

Table 1 Tensile property of metallic alloys

Material	**Yield strength ($R_{p0.2}/MPa$)**	**Tensile strength (R_m/MPa)**	**Elongation (%)**	**Reduction of area (%)**
40CrNi2Si2MoVA	1643	1950	12	53
16Co14Ni10Cr2Mo	1482	1620	12	60
30CrMnSiNi2A	1141	1653	15	47
0Cr13Ni8Mo2Al	1432	1484	11	58

Table 1 Tensile property of metallic alloys

Material	Yield strength ($R_{p0.2}$/MPa)	Tensile strength (R_m/MPa)	Elongation (%)	Reduction of area (%)
2124-T851	400	440	11	40
7475-T7351	450	528	13	44
7050-T7451	470	539	14	38
TC21	1003	1103	16	31
Ti60	960	1025	14	28

The parameters of shot peening processes are shown in Table 2

Table 2 Shot peening parameters of high-strength structural materials

Material	Shot	Intensity(mm)	Coverage (%)	Air pressure (MPa)
40CrNi2Si2MoVA	S330	0.40	100	0.35
16Co14Ni10Cr2Mo	S330	0.30	100	0.25
30CrMnSiNi2A	S330	0.30	100	0.25
0Cr13Ni8Mo2Al	BZ15	0.15	100	0.20

Table 2 Shot peening parameters of high-strength structural materials

Material	Shot	Intensity(mm)	Coverage (%)	Air pressure (MPa)
7475-T7351	S110	0.20	200	0.25
7050-T7451	S110	0.20	200	0.25
TC21	BZ20	0.15	200	0.20
Ti60	BZ20	0.15	200	0.20

Measuring residual stresses

- X-ray diffraction method:
- X3000 type
- Proto LXRD type
- μ-X360s type X-ray diffraction stress testers
- Step-by-step electro-polishing method

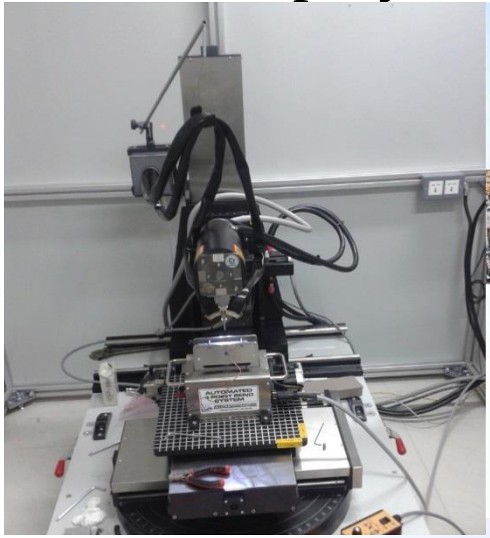

The typical profile of residual stress along the depth

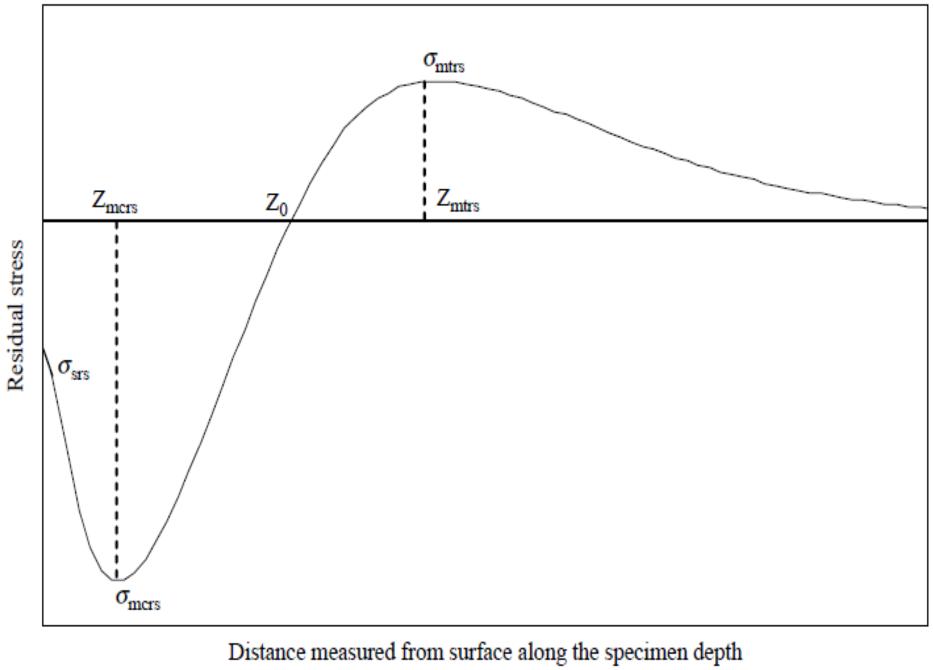

Figure 1. Schematic surface strengthening residual stress field and its parameters

(1) σ_{srs} – surface residual stress;
(2) σ_{mcrs} – the maximum compressive residual stress;
(3) σ_{mtrs}– the maximum tensile residual stress;
(4) Z_{mcrs} – distance from surface, where the compressive residual stress is maximum;
(5) Z_0– depth at which the residual stress becomes zero and beneath where the residual stress is tensile;
(6) Z_{mtrs} – distance from surface, where the tensile residual stress is maximum.

The characteristic parameters of residual stress fields for these high-strength metallic materials are also listed in Table 3.

Table 3 Characteristic parameters of residual stress fields for high-strength materials induced by shot or laser peening.

Material	σ_{srs} (MPa)	σ_{mcrs} (MPa)	σ_{mtrs} (MPa)	Z_{mcrs} (μm)	Z_0 (μm)	Z_{mtrs} (μm)
40CrNi2Si2MoVA	-825	-1500	327	40	280	315
16Co14Ni10Cr2Mo	-880	-1000	204	80	300	348
30CrMnSiNi2A	-840	-1150	304	75	450	508
0Cr13Ni8Mo2Al	-883	-1180	148	35	125	214
2124-T851	-210	-275	90	42	260	308

Table 3 Characteristic parameters of residual stress fields for high-strength materials induced by shot or laser peening.

Material	σ_{srs} /MPa	σ_{mcrs} /MPa	σ_{mtrs} /MPa	Z_{mcrs} /μm	Z_0 /μm	Z_{mtrs} /μm
7475-T7351	-308	-380	73	45	300	370
7050-T7451 shot peening	-225	-378	58	100	280	304
Laser peening	-350	-350		0	1800	
TC21	-420	-618	134	60	220	262
Ti60	-450	-646	158	50	220	243

Fatigue tests

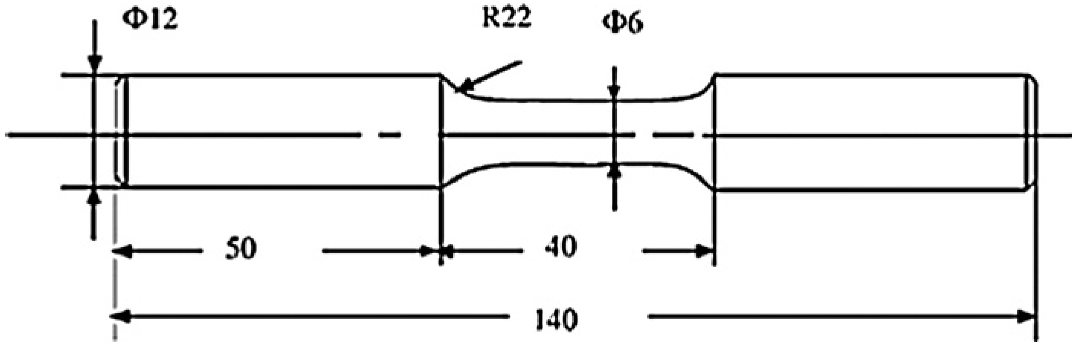

- Rotating bending fatigue tests (R=-1)
- Three-point bending tests (R=0.1)
- Determine the fatigue strengths/limits for each alloy at 1×10^7 cycles by a staircase method

(The experimental results are shown in Table 4)

同濟大學 TONGJI UNIVERSITY

Table 4 Fatigue strengths/limits of smooth specimens of high-strength structural materials

Material	**Surface condition**	σ_{app} **(MPa)**	σ_{loc} **(MPa)**	σ_{sur} **(MPa)**	σ_{int} **(MPa)**	**Increscent**
40CrNi2Si2MoVA	Machining Shot peening	718 1040	750 1065	750	1065	1.42
16Co14Ni10Cr2Mo	Machining Shot peening	720 835	720 966	720	966	1.34
30CrMnSiNi2A	Machining Shot peening	763 887	738 997	738	997	1.35
0Cr13Ni8Mo2Al	Machining Shot peening	550 720	580 783	580	783	1.35

Table 4 Fatigue strengths/limits of smooth specimens of high-strength structural materials

Material	Surface condition	σ_{app} (MPa)	σ_{loc} (MPa)	σ_{sur} (MPa)	σ_{int} (MPa)	Increscent
2124-T851	Machining Shot peening	160 206	160 224	160	224	1.40
7475-T7351	Machining Shot peening	185 223	185 252	185	261	1.41
7050-T7451	Machining Shot peening	263 170	261 150	185	206	1.37
TC21	Machining Shot peening	160 206	560 430	400	560	1.40
Ti60	Machining Shot peening	416 580	430 580	430	594	1.38

The fatigue sources were determined by SEM.
The typical fatigue sources are shown in Figure 2.

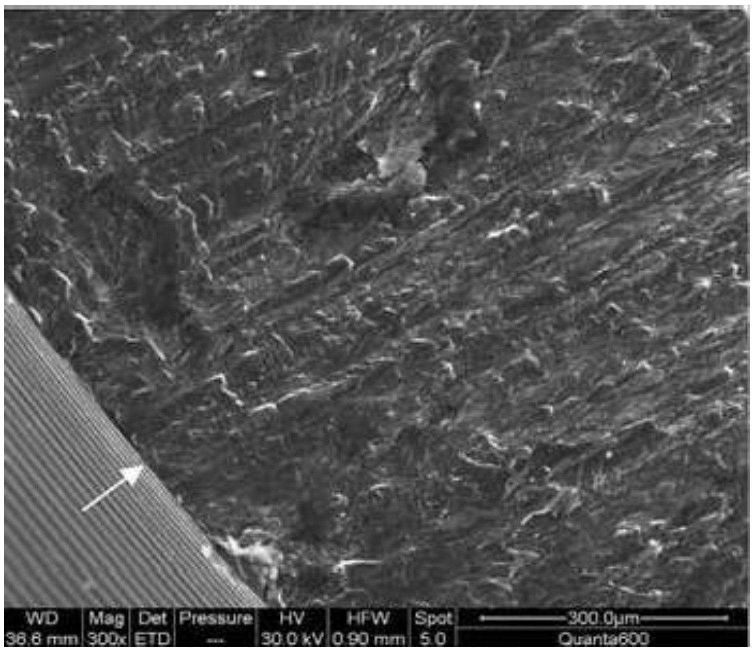

(a)

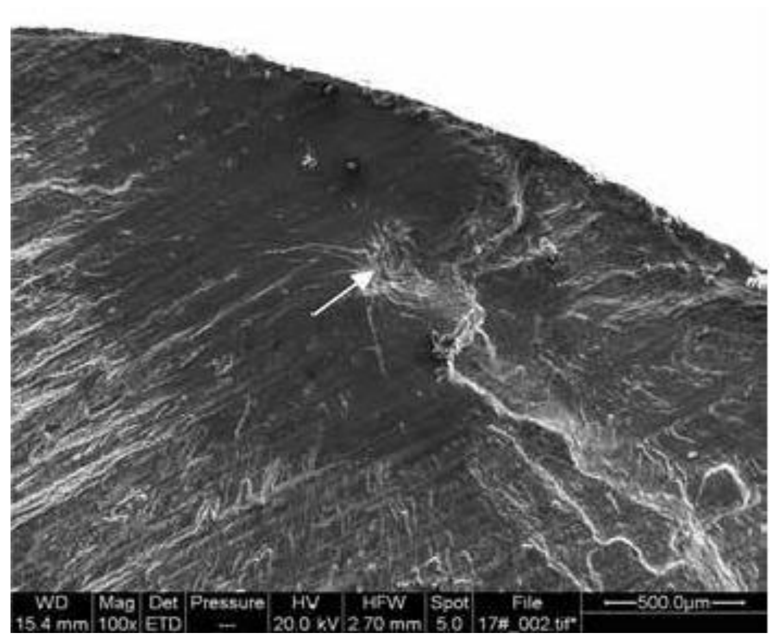

(b)

Figure 2. Typical fatigue crack Locations (a) Machined specimen of 7050-T7451 aluminum alloy; (b) shot-peened specimen of 7050-T7451 aluminum alloy; (c) machined specimen of Ti60 titanium alloy; (d) shot-peened specimen of Ti60 titanium alloy; (e) shot-peened specimen of TC21 titanium alloy; (f) fatigue cracks in the source of (e) .

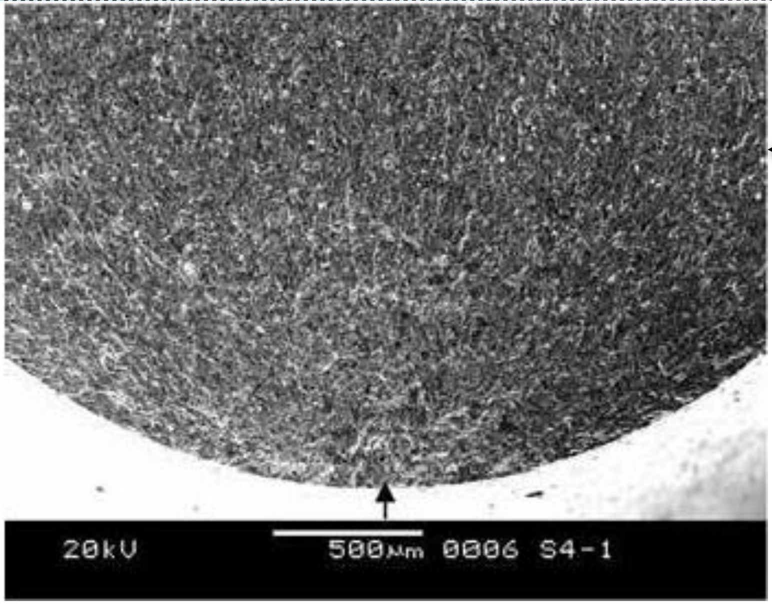
20kV
500µm 0006 S4-1

(c)

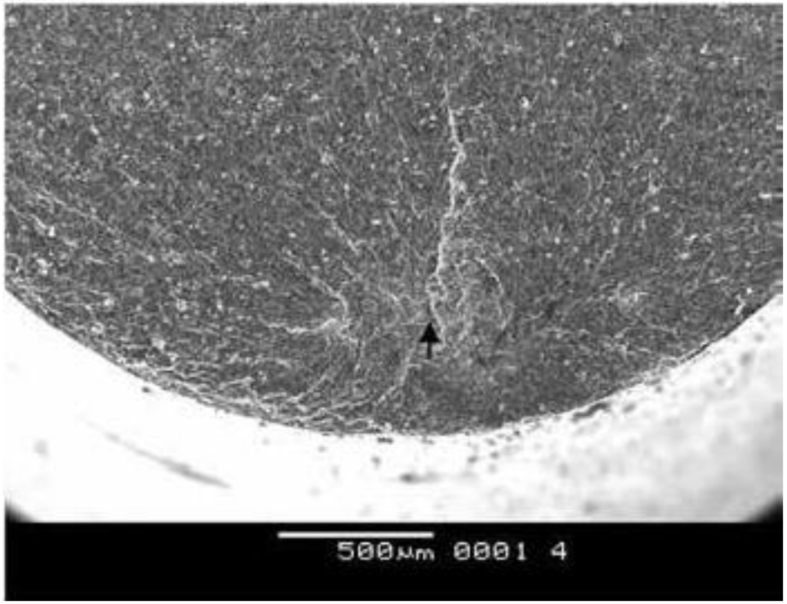
500µm 0001 4

(d)

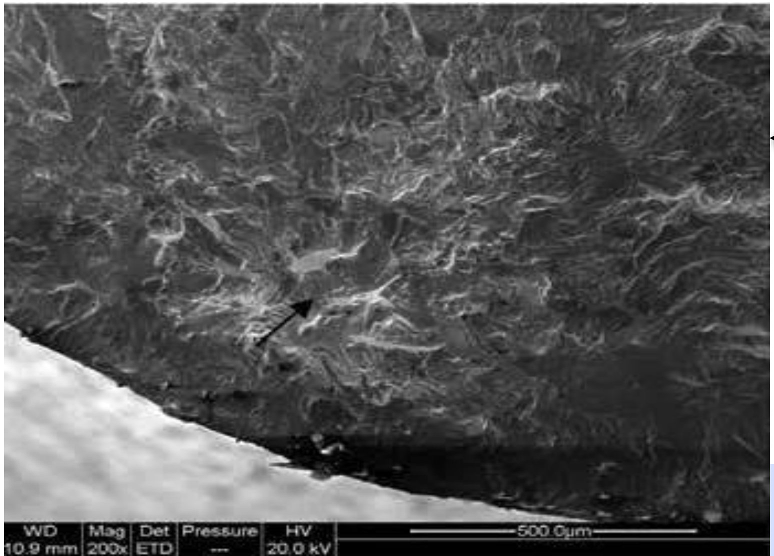
WD 10.9 mm
Mag 200x
Det ETD
Pressure ---
HV 20.0 kV
500.0µm

(e)

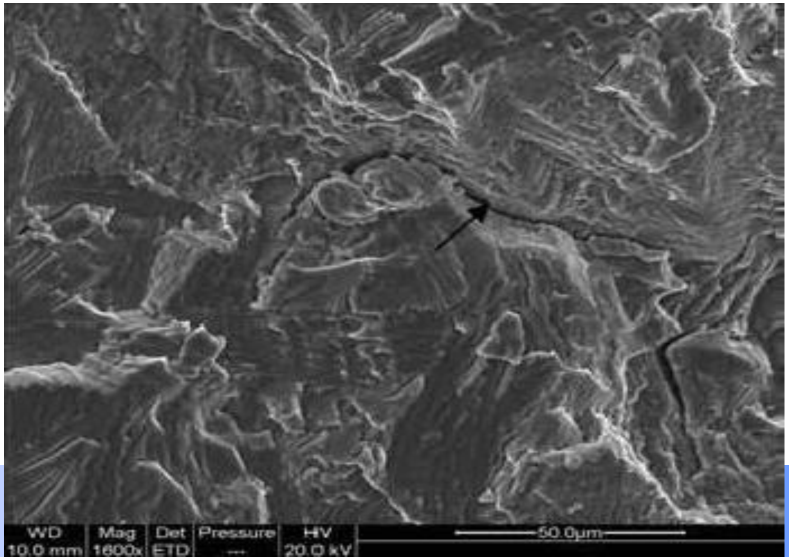
WD 10.0 mm
Mag 1600x
Det ETD
Pressure ---
HV 20.0 kV
50.0µm

(f)

同濟大學 TONGJI UNIVERSITY

2.2 Fatigue strength or fatigue limits of shot-peened smooth fatigue specimens after or before different surface treatments

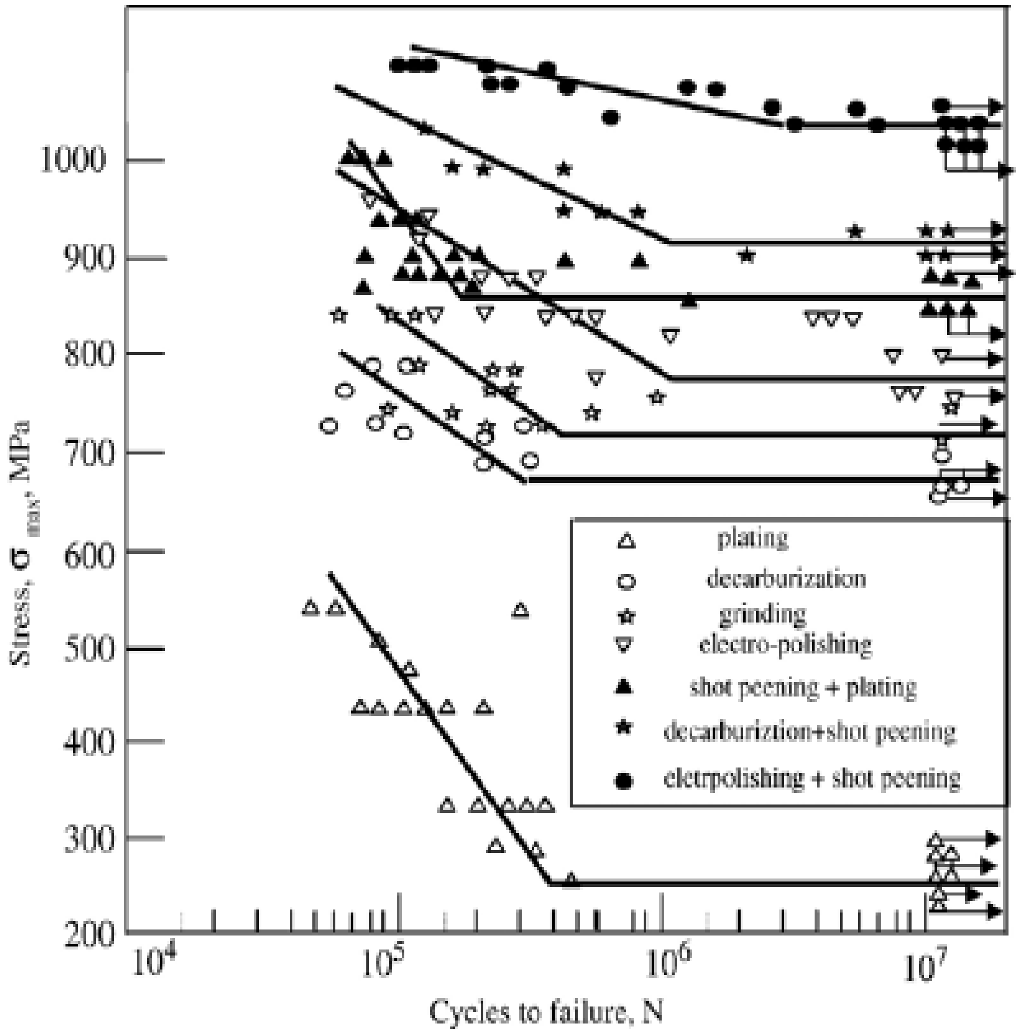

The fatigue S-N curves of specimens with different final surface conditions are shown in Fig. 3.

ELSEVIER
Available online at www.sciencedirect.com
ScienceDirect
Materials Letters 61 (2007) 466–469
materials letters
www.elsevier.com/locate/matlet

Influence of surface integrity on fatigue strength of 40CrNi2Si2MoVA steel

Yu-kui Gao [a,*], Xiang-bin Li [a], Qing-xiang Yang [b], Mei Yao [b]

Fig. 3. S–N curves of 40CrNi2Si2MoVA steel with different final surface conditions.

The values of the fatigue limit σ_{-1} for 1×10^7 cycles are also listed in Table5.

Table 5 Final surface conditions and fatigue limits of 40CrNi2Si2MoVAstaire specimens

No.	**Final surface condition**	**Rz/μm**	σ_{srs}**/MPa**	σ_{mcrs}**/MPa**	δ_0**/mm**	σ_{-1}**/MPa**
1	Grinding	3.5~3.8	-400	-600	0.12	718
2	Grinding+electropolishing	2.8~3.2	-80	-120	0.08	780
3	Electropolishing+decarburization	3.0~3.2	-320	-400	0.16	674
4	Hard chromium	3.2~3.8	580	800	0.23	270
5	Grinding+shot peening	4.8~5.0	-920	-1200	0.26	1040
6	Decarburinzation+shot peening	5.0~5.3	-700	-850	0.23	920
7	Shot peening+hard chromium	2.8~3.0	-720	-940	0.26	840

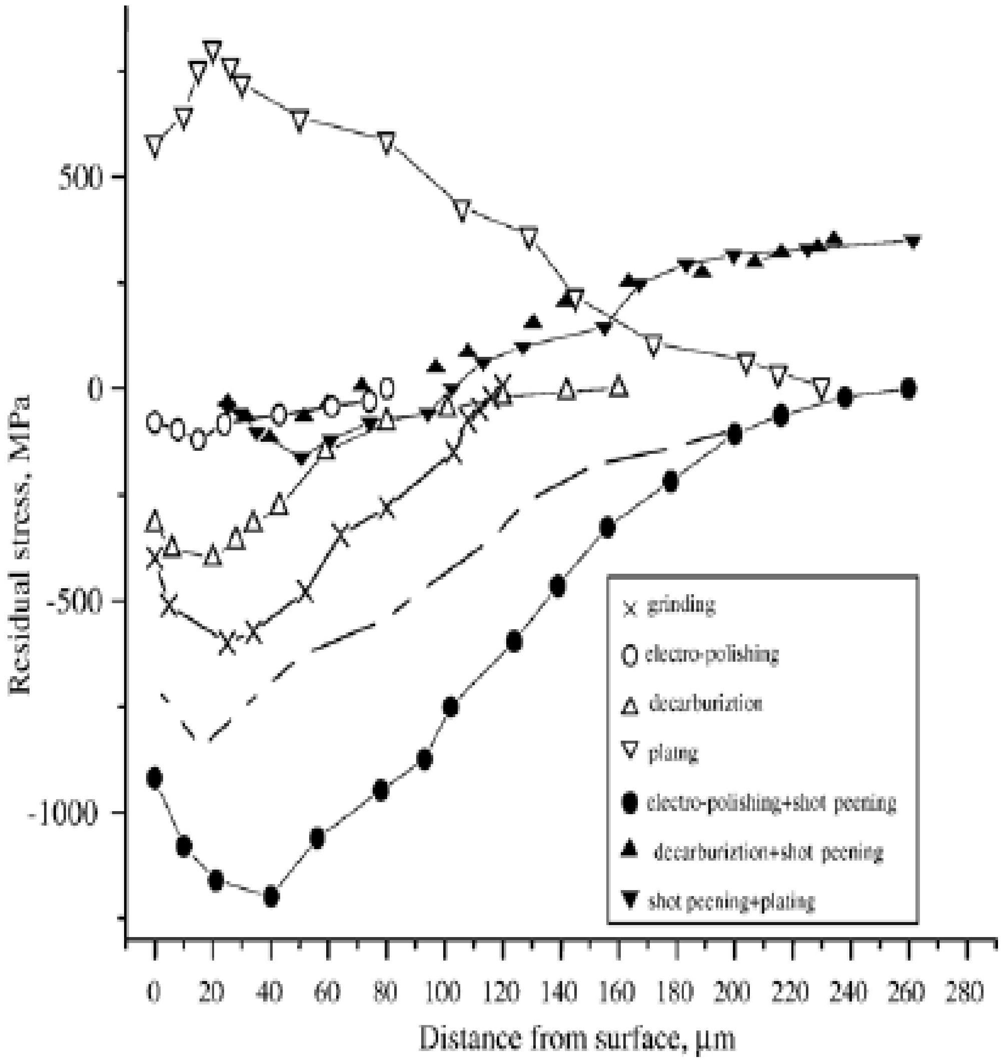

The residual stress fields of different groups of specimens are shown in Fig. 4.

Fig. 4. Residual stress fields in a surface layer.

Fracto-graphical analysis shows that the fatigue crack source is also located in the interior for shot peened and then plated specimen (Fig. 5).

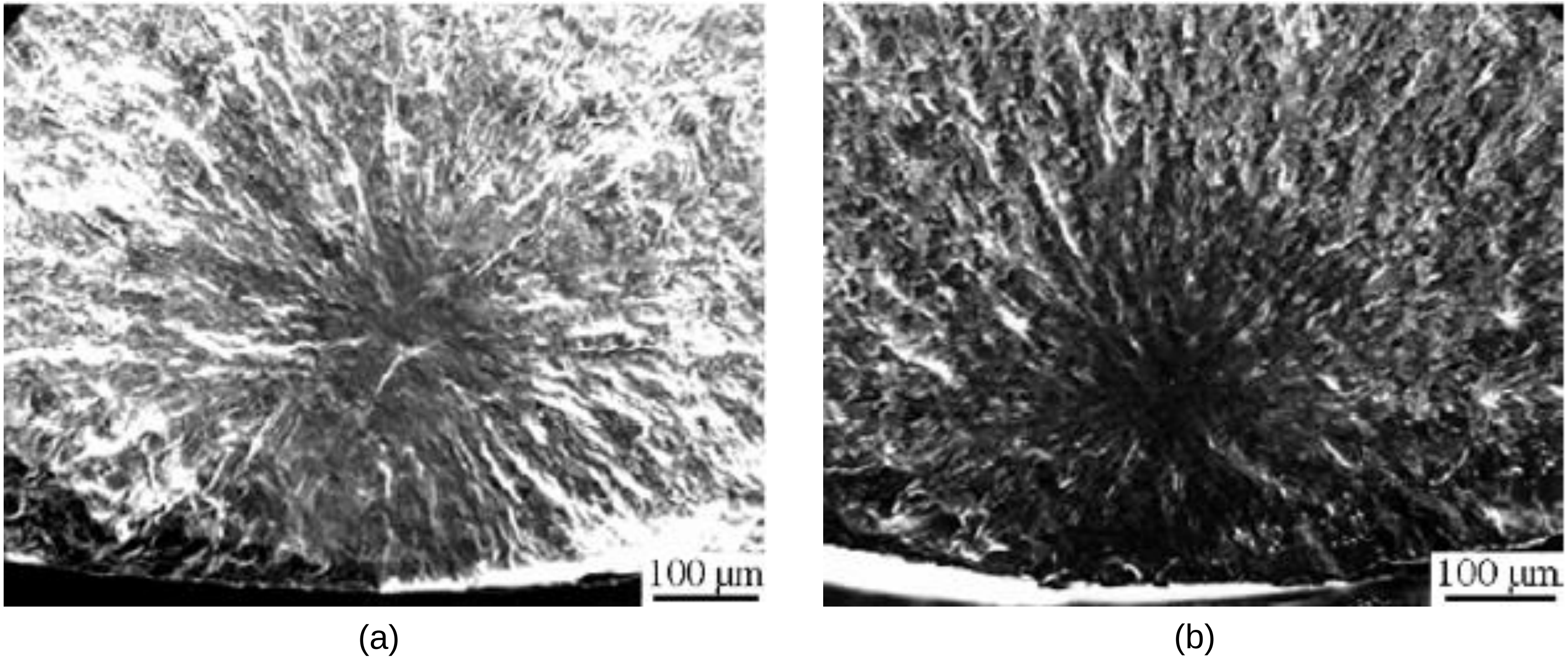

Fig. 5. Fatigue fracto-graphs of specimens. (a) After electro-polishing and shot peening, and (b) after shot peening followed by plating.

Hard chromium plating

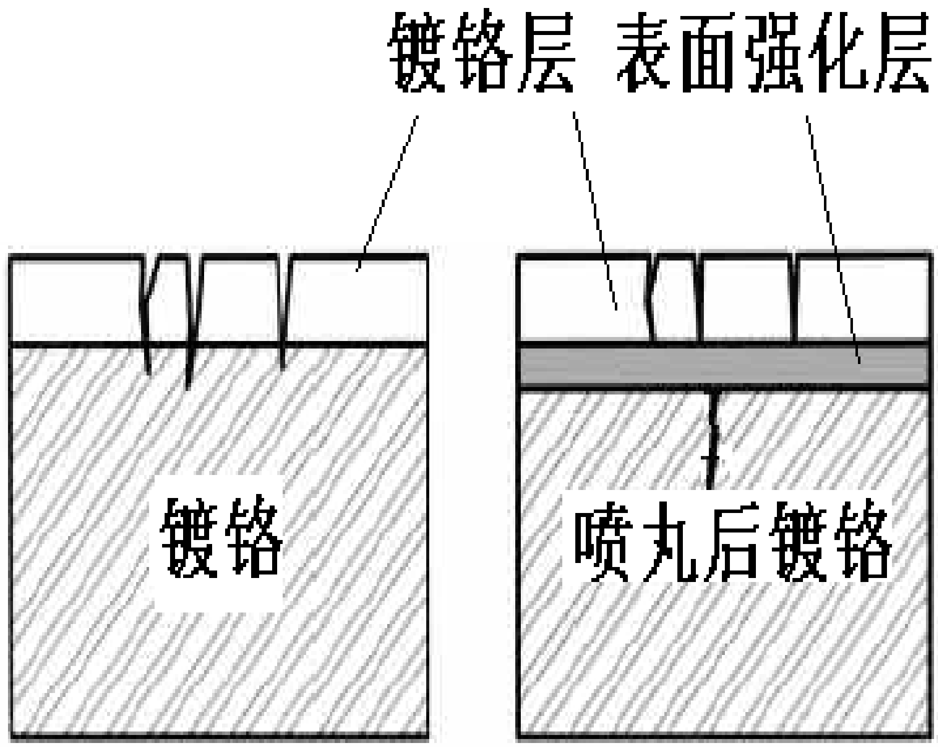

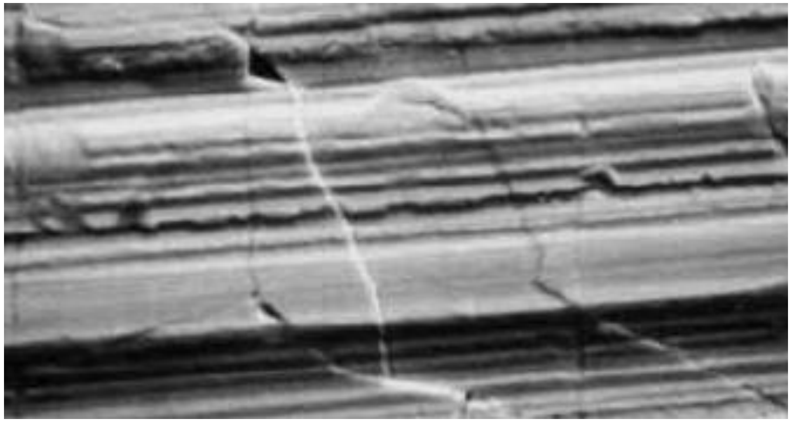

2.3 Small crack propagation and fatigue life in residual stress fields caused by shot peening

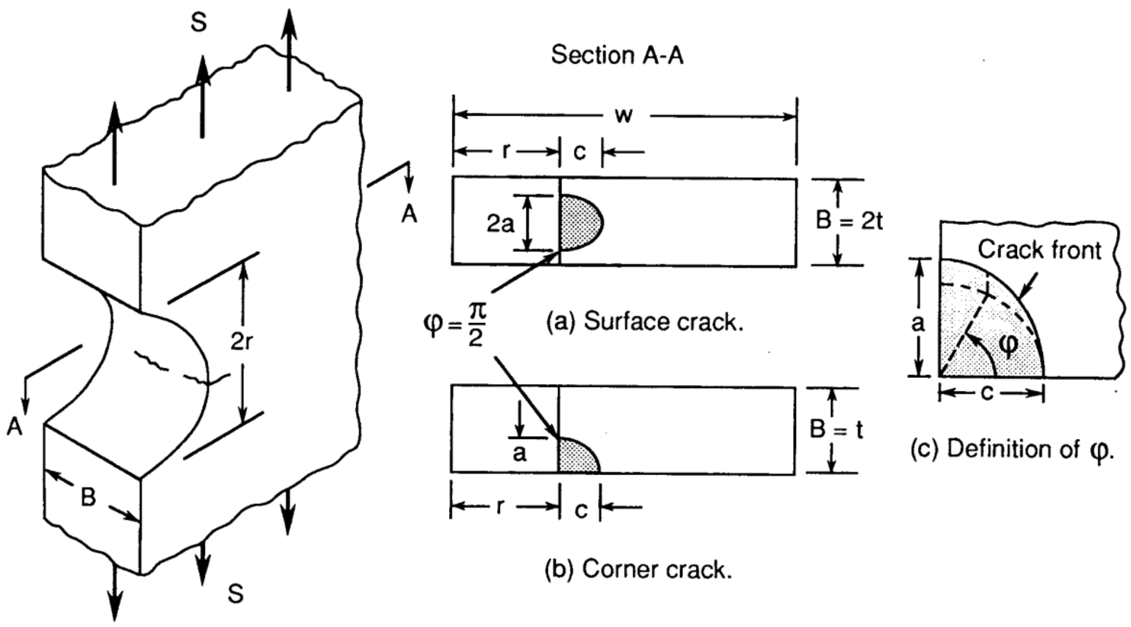

- Data for the lengths of small cracks as a function of loading cycles were recorded using AC paper replicas.
- Typical replica images by SEM showing the crack length after different numbers of cycles are shown in Figs. 6 and 7 for un-peened and shot peened specimens, respectively.

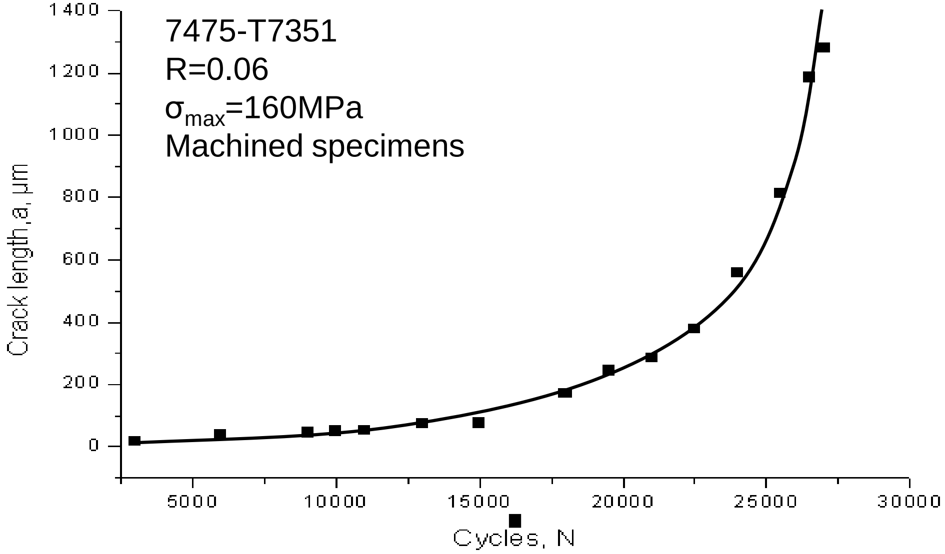

7475-T7351
R=0.06
σmax=160MPa
Machined specimens
Crack length,a,μm
Cycles, N

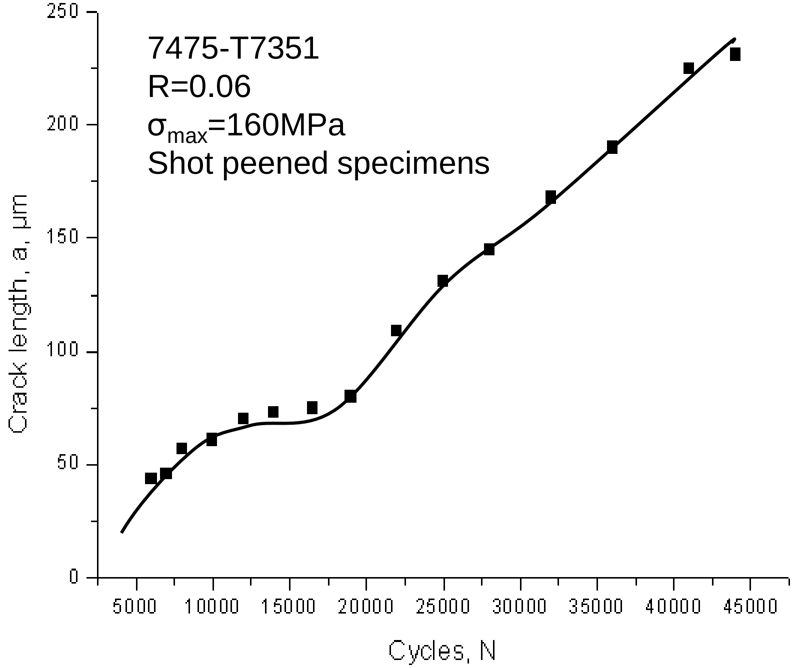

7475-T7351
R=0.06
σmax=160MPa
Shot peened specimens
Crack length, a, μm
Cycles, N

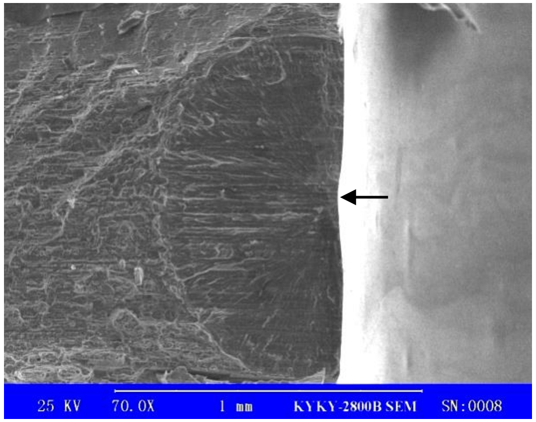

25 KV 70.0X 1 mm KYKY-2800B SEM SN:0008

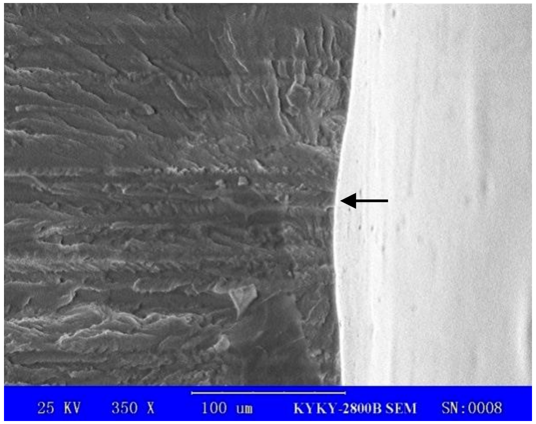

25 KV 350 X 100 um KYKY-2800B SEM SN:0008

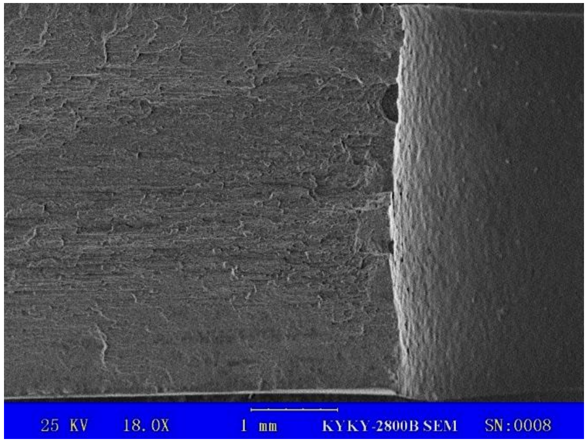

25 KV 18.0X 1 mm KYKY-2800B SEM SN:0008

Unpeened specimen

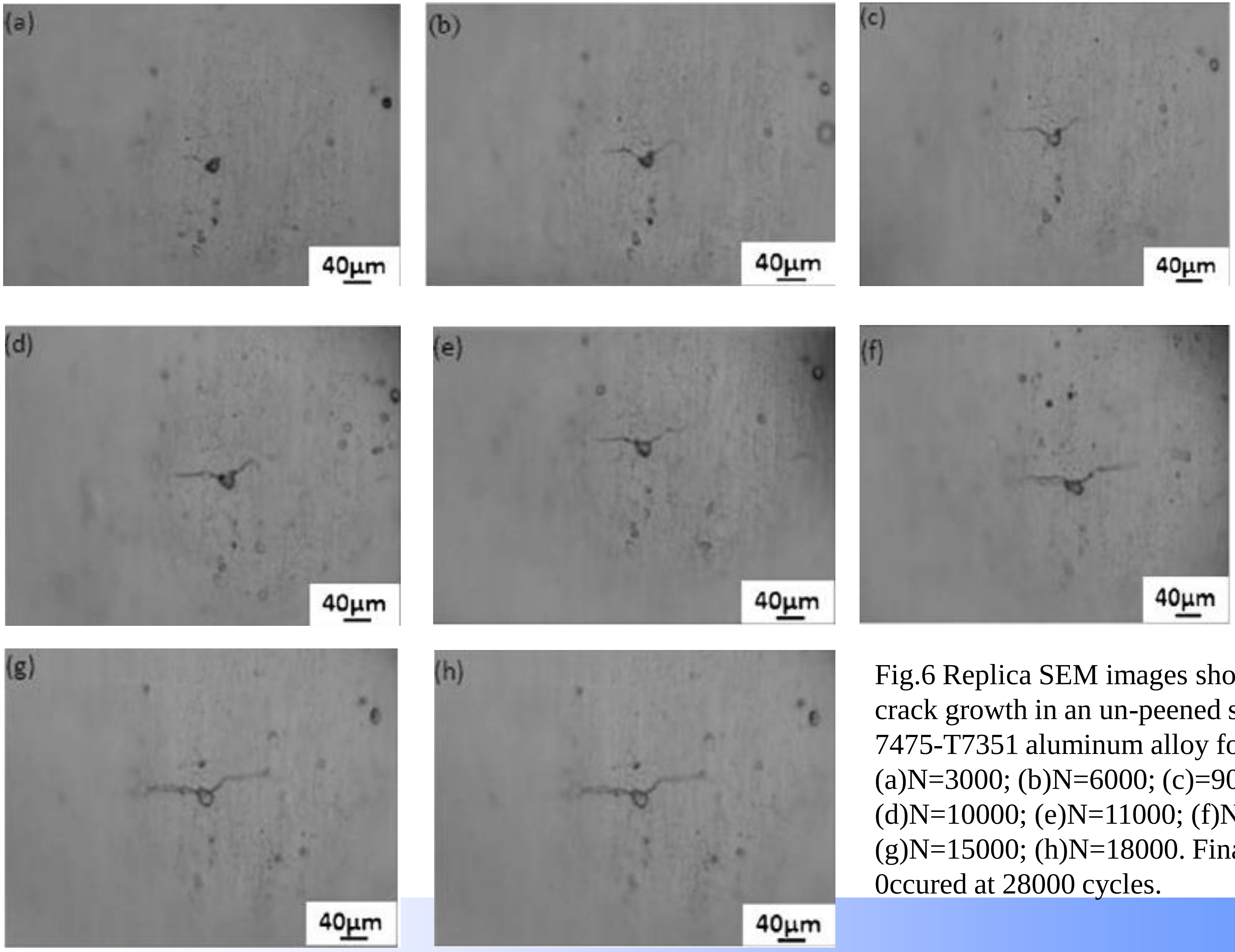

Fig.6 Replica SEM images showing small crack growth in an un-peened specimen of 7475-T7351 aluminum alloy for N cycles (a)N=3000; (b)N=6000; (c)=9000; (d)N=10000; (e)N=11000; (f)N=13000; (g)N=15000; (h)N=18000. Final failure 0ccured at 28000 cycles.

Shot peened specimen

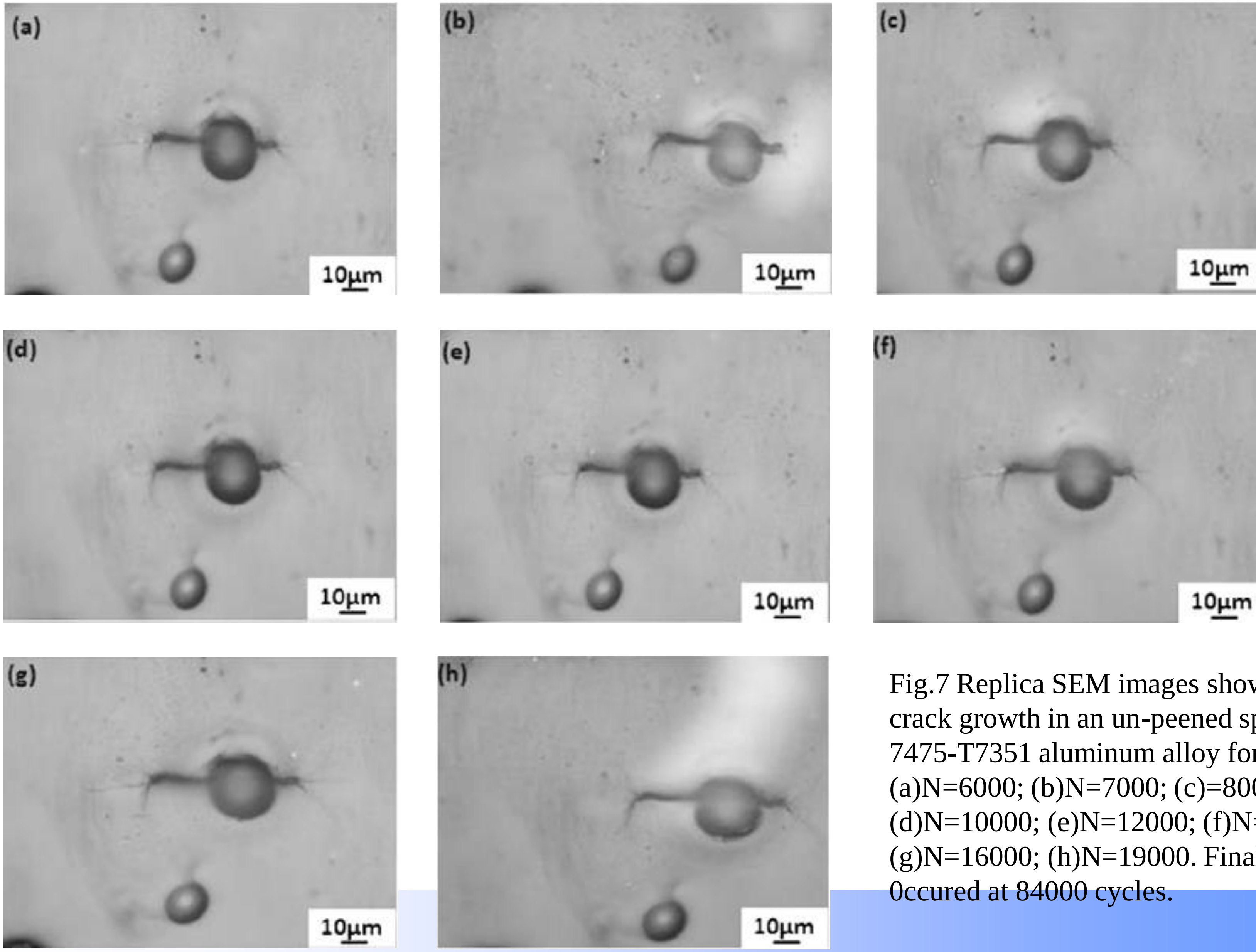

Fig.7 Replica SEM images showing small crack growth in an un-peened specimen of 7475-T7351 aluminum alloy for N cycles (a)N=6000; (b)N=7000; (c)=8000; (d)N=10000; (e)N=12000; (f)N=14000; (g)N=16000; (h)N=19000. Final failure 0ccured at 84000 cycles.

- small cracks appeare very early during cycling
- the crack initiation life is only a very small part of the total fatigue life
- the use of a total fatigue life approach is based on small crack growth analysis
- fatigue cracks initiate from second phase particles and grow from both sides of the defects

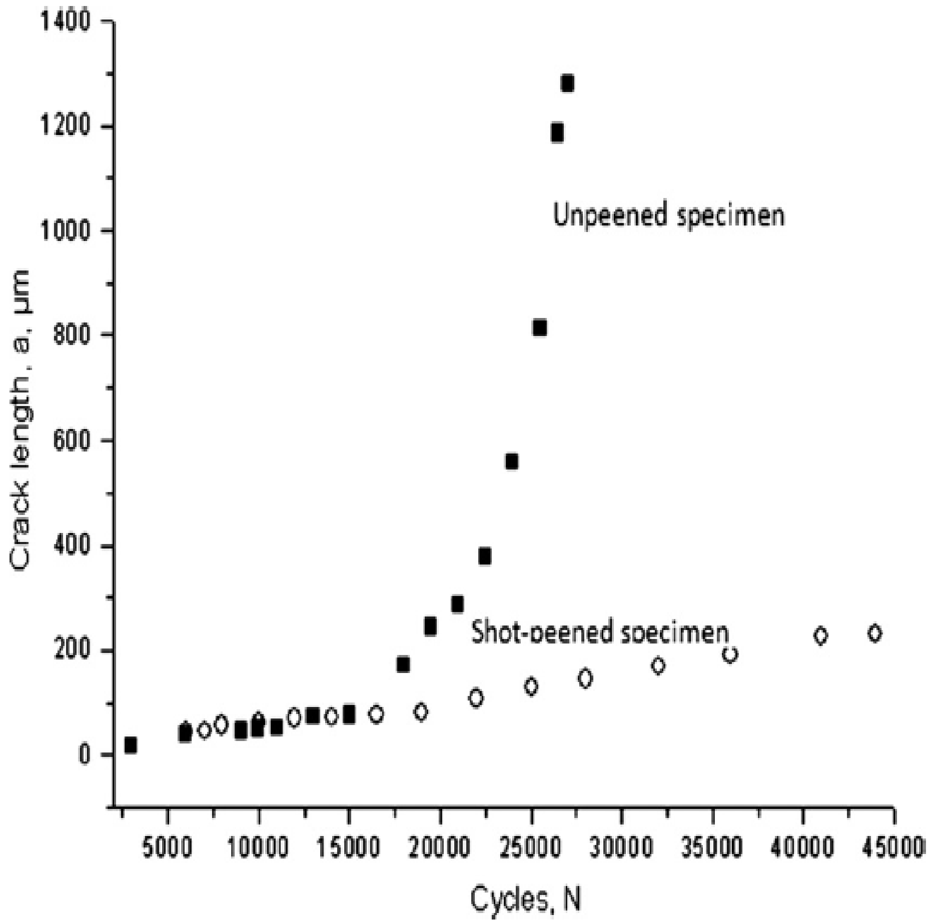

Compared with the un-peened specimens, cracks in the shot peened specimens grow much more slowly, as shown in Fig.8, especially cracks longer than 80μm.

Fig.8 Crack length vs. number of cycles for small cracks in 7475-T7351 aluminum alloy, showing the effect of shot peening.

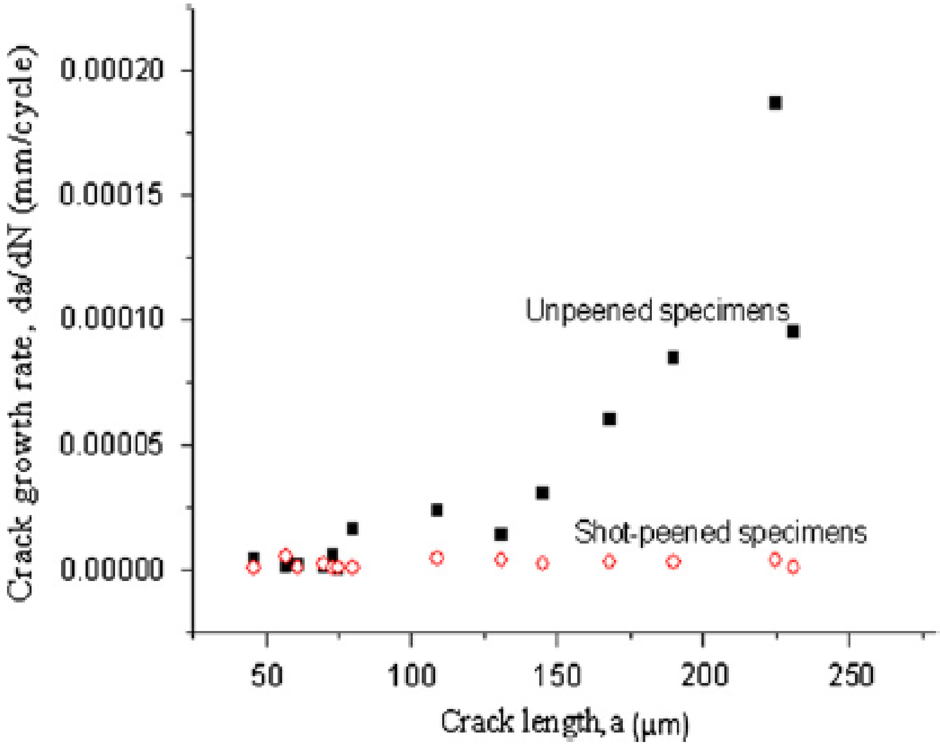

The corresponding small crack growth rates as a function of crack length are shown in Fig.9. Compared with un-peened specimens, the small crack growth rates are very much lower for shot peened specimens. The difference increases rapidly with increasing crack length.

Fig.9 Crack growth rates (da/dN) vs. crack length (a) for small cracks in 7475-T7351 aluminum alloy with and without shot peening.

3.1 Fatigue crack initiation and fatigue strength/fatigue limit

Compare

Un-surface-strengthened specimens

- fatigue sources locate at the surface
- surface fatigue strength/limit

Surface-strengthened specimens

- fatigue sources located beneath the surface-enhanced layer
- subsurface or internal fatigue strength/limit
- the critical stress for initiation of fatigue crack in the interior should be higher than that at the surface

The transfer of the fatigue crack source from surface into interior may be another mechanism for the improvement of apparent fatigue limit of shot peened specimens.

Formation of fatigue crack source

1. Dislocation motions within a few weak grains, which will soon be restricted by their surrounding grains.
2. Harmonizing dislocation motions in the surrounding grains, which allow the further dislocation motions in the weak grains.
3. Reverse motion of dislocations in individual weak grains, especially along some favorite slip bands, caused by the restraining effect from surrounding grains during unloading, or under the action of the applied stress during reverse loading.
4. Formation of persistent slip bands with concentrated plastic strain in the weak grains after repeated loading and followed by the presence of "cyclic meso-yielding areas", as shown in Figure 3.
5. Formation of fatigue cracks from "cyclic meso-yielding areas", which will soon be arrested by grain boundaries, along the persistent slip bands.
6. Propagation of one of the initial main cracks across grain boundaries, which should be considered probabilistic.

The dominant process during fatigue source evolution is to form “cyclic meso-yielding areas”.

Hall and Petch equation:

$$\sigma_w = \sigma_0 + k_w d^{-1/2}$$

σ_w--fatigue strengths / limits of a metal

σ_0--the stress impeding the dislocation motion along the slip plane within weak grains

k_w--a coefficient reflecting the resistance to cause the dislocation motion “spread across” the grain boundary into the adjacent grains

d--the average grain diameter

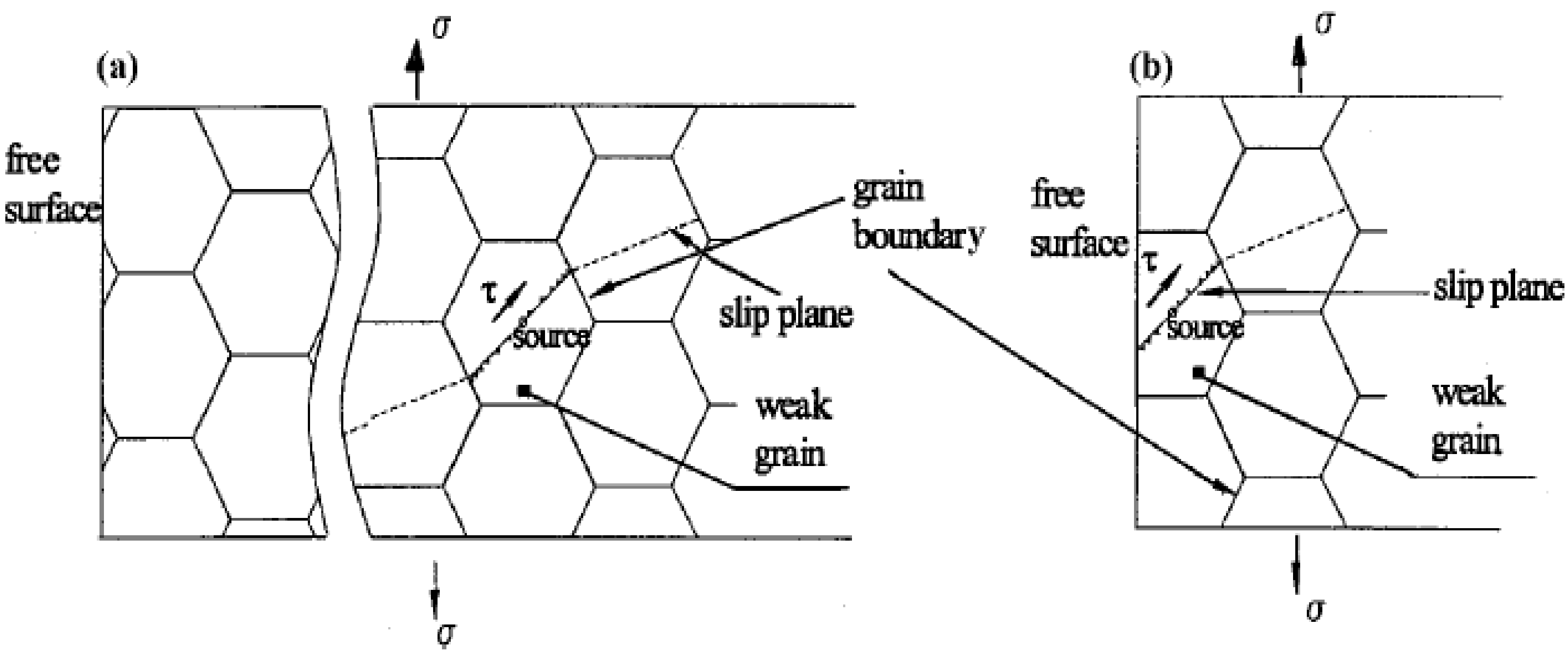

Fig. 10 Schematic diagram of meso-yielding in (a) the interior, and (b) at surface.

- σ_w is much lower than σ_y
- the dislocation motion in subsurface or internal grains is restricted by the neighboring grains from different sides, while that in the surface grains is only restricted from the internal side and is free from its surface side
- k_w , as well as σ_w should be higher for a weak grain located in the interior than that for a weak grain at or near the surface

Surface enhancement is maybe related to the improved yield strength of surface layer and compressive residual stresses induced by surface enhancements.

Internal fatigue limit

$$\sigma_{wi} = \sigma_{pi} + \sigma_{ri}$$

σ_{pi} --the local applied stress of specimen at the position of fatigue crack source

σ_{ri} --the local (tensile) residual stress at the position of fatigue crack source

- This mechanism for improvement of apparent fatigue limit of shot-peened specimens is different from, but not contrary to the generally accepted mechanism, according to which the improvement of apparent fatigue limit of shot-peened metallic parts is directly attributed to the decrease of mean stress of the applied stress cycle due to the induced compressive residual stress.
- The apparent fatigue limit should be related to the surface fatigue limit of metal as well as the compressive residual stress in the surface layer.

3.2 Fatigue crack propagation and fatigue life prediction

Fig. 11 demonstrates that the small cracks are all surface cracks and that the crack length in the thickness direction, is similar to the crack length in the width direction, therefore da/dN = dc/dN.

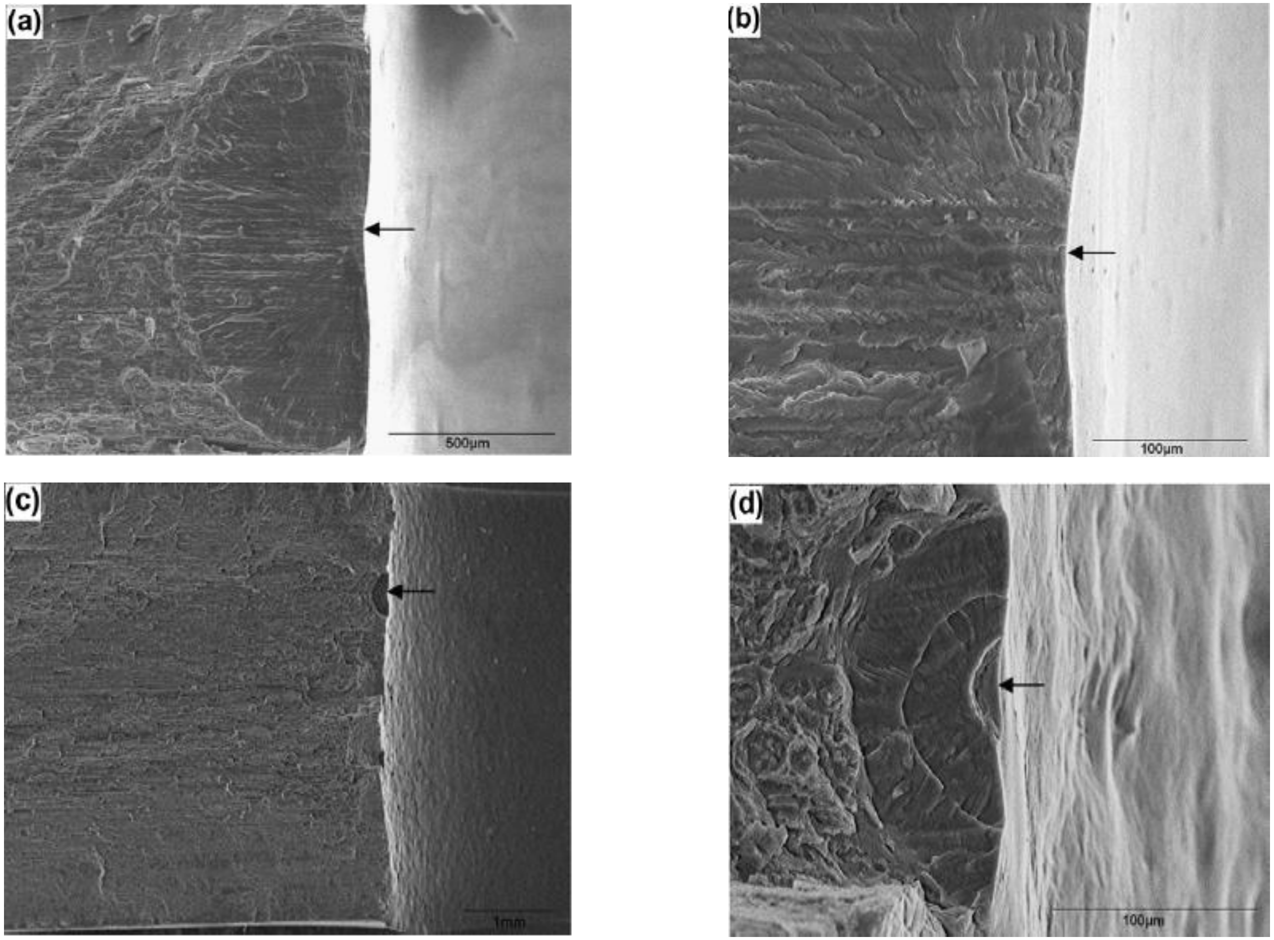

Fig.11 SEM fracture surfaces of (a and b) un-peened and (c and d) shot peened specimens.

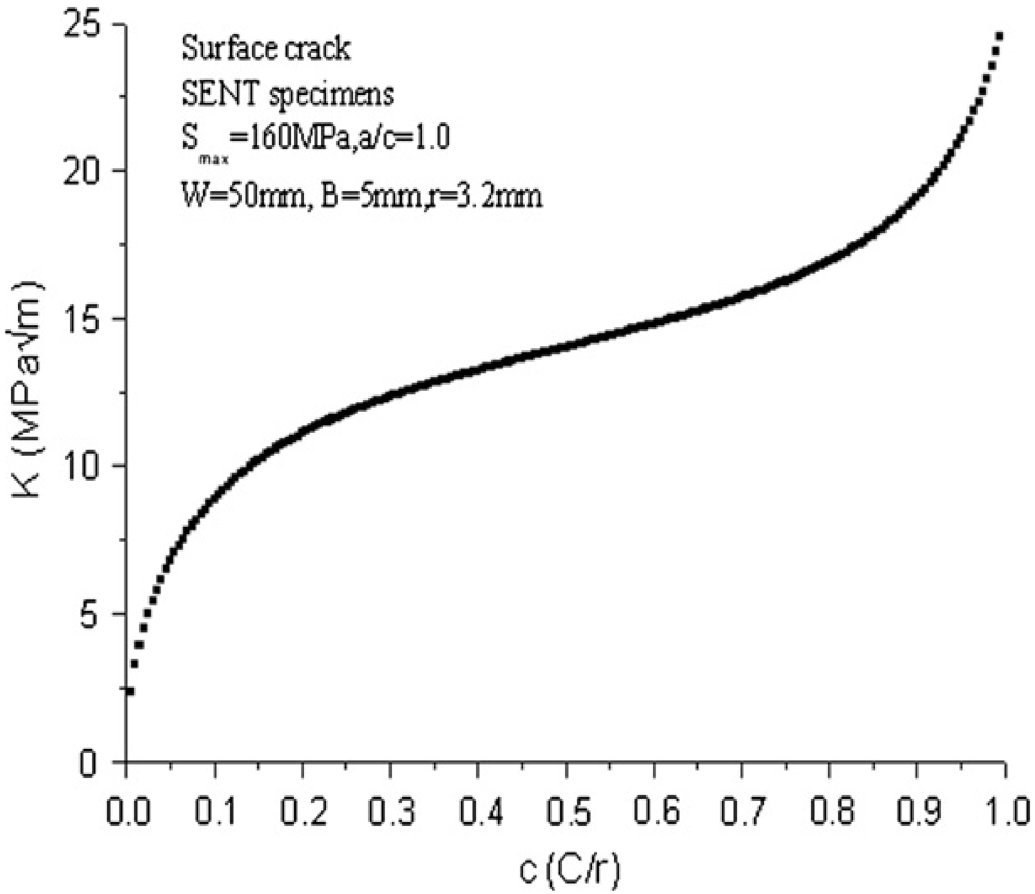

To analyze the effect of shot peening on small crack growth, SIFs must be known for cracks for cracks subjected to both external loads and residual stresses.

SIFs calculated using the 3-D weight function method for small surface cracks in un-peened specimens loaded by a uniform external tensile stress S_{max}=160 Mpa are given in Fig.12.

Fig. 12. 3-D SIFs for a surface crack in an un-peened specimen under uniform tension (S = 160 MPa).

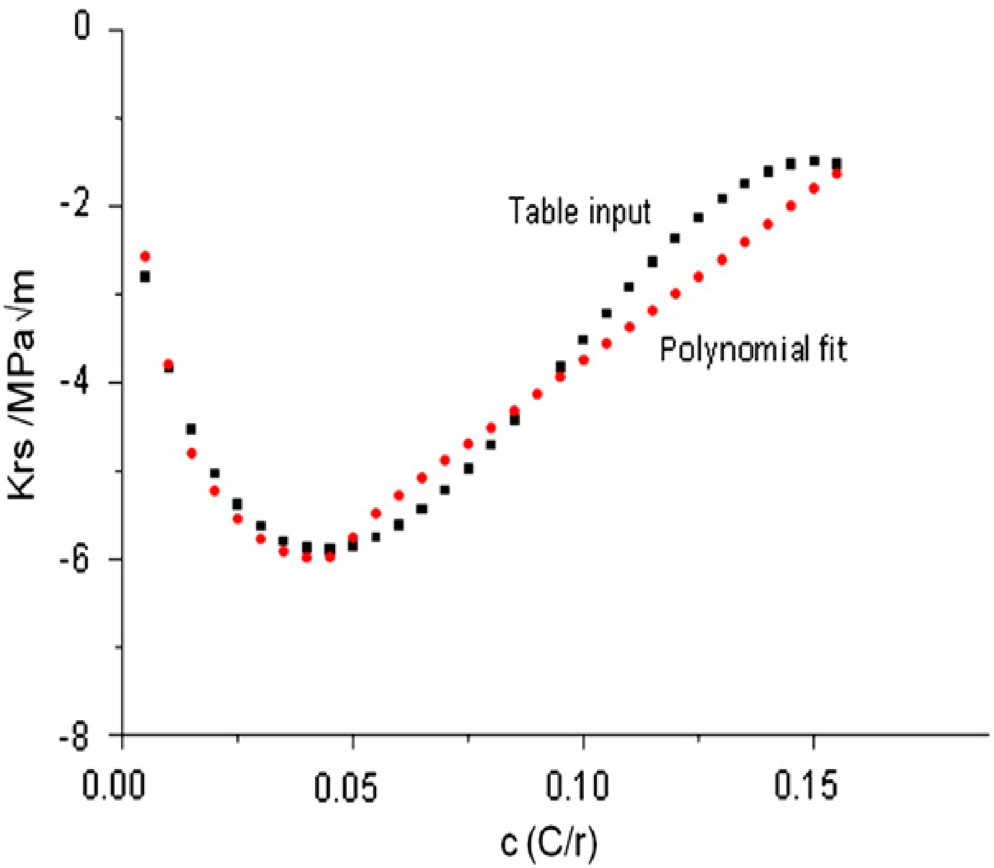

The 2-D edge crack SIFs under the condition of shot peening-induced residual stresses as calculated by both of these methods are shown in Fig. 13.

Fig. 13. Stress intensity factors for a 2-D edge crack subjected to shot peening residual stresses

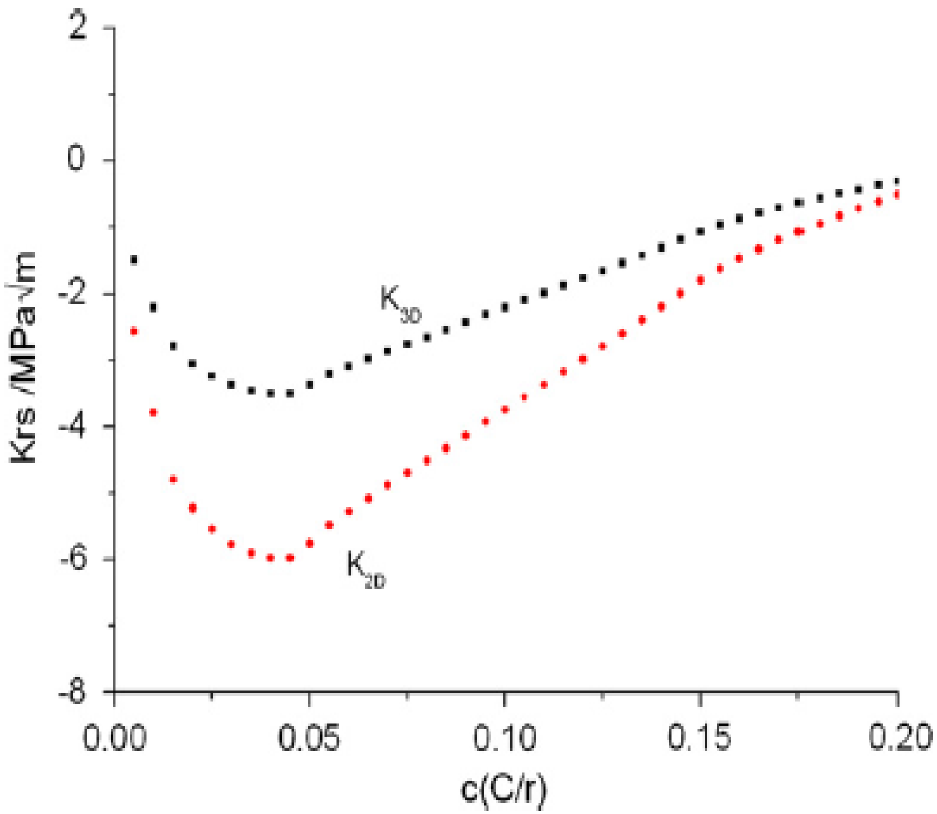

To determine the 3-D SIFs from the corresponding 2-D SIFs we employ an analogy by taking the ratio between the 3-D SIFs for surface cracks and the 2-D edge crack SIFs for the case of a uniform tension stress and then use this known ratio to obtain the 3-D SIFs for the case of residual stresses.

Fig.14 2-D and 3-D SIFs in the presence of shot peening residual stresses.

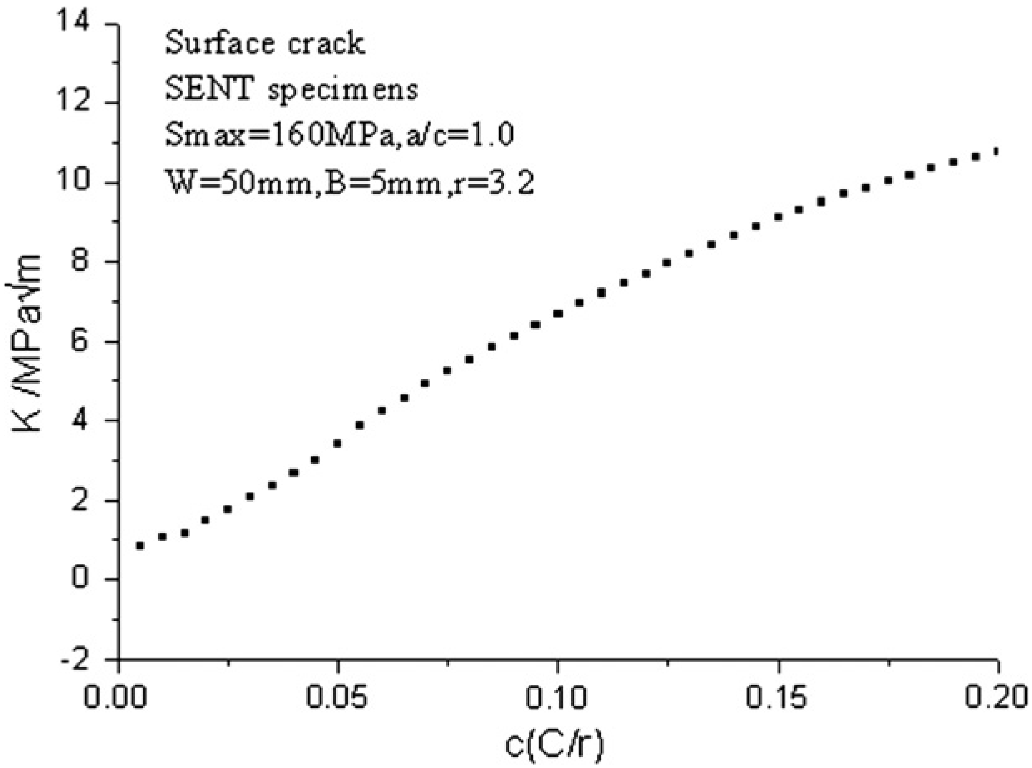

By superposition, the surface crack SIFs subjected to both the applied load and the residual stresses are obtained (Fig. 17).

Fig. 15. Surface crack SIFs for shot peened specimens subjected to a combination of uniform tension Smax = 160 MPa and residual stresses.

3.3 Fatigue life prediction

Small crack theory

- how to accurately determine the residual stress distribution caused by shot peening

---X-ray diffraction methods, neutron scattering and synchrotron radiation techniques

- how to calculate stress intensity factors (SIFs) for cracks in residual stress fields with steep gradients in the material surface layer

---weight function method

Compressive residual stress field

The CRSF introduced by shot peening is dependent on both the mechanical properties of target and peening regime.

$$\sigma_{mcrs} = 0.86\sigma_{0.2} - 51$$

$$\sigma_{srs} = R(114 + 0.563\sigma_{0.2})\ (R = 0.997\sim1.13)$$

$$Z_0 = (1.41D_d - 0.09S)[1 + 0.09(C-1)^{0.55}]$$

$$Z_m \approx 0.28Z_0$$

σ_{mcrs} =the maximum compressive residual stress (MPa)

σ_{srs}=surface residual stress (MPa)

Z_0=depth of compressive residual stress field (μm)

Z_m =distance from surface, to the location of maximum compressive residual stress (μm)

The calculation of stress intensity factor

$$K = \int_0^A m(A,X)\sigma(X)dX$$

m(A, X)—weight function

where A and X are the crack length and the coordinate along the crack, respectively

σ—a scaling factor with the dimension stress

W — a characteristic length parameter

Here we let W = r, the notch radius of the SENT specimens. The above equation therefore has the form:

$$K = f\sigma\sqrt{\pi A} \qquad f = \int_0^a \frac{\sigma(x)}{\sigma}\frac{m(a,x)}{\sqrt{\pi a}}dx \qquad x=X/r,\ a=A/r$$

Fatigue crack closure

Small crack growth rates and fatigue lives of naturally occurring small cracks in shot peened and un-peened specimens were calculated using small crack theory and a crack closure model.

The applied stress intensity factor is:

$$\Delta \mathrm{K} = K_{max} - K_{min}$$

K_{max}--the maximum stress intensity factor
K_{min}--the minimum stress intensity factor

The efficient stress intensity factor is:

$$\Delta K_{eff} = K_{max} - K_{op}$$

K_{op} --open stress intensity factor

Crack closure coefficient is:

$$U = \frac{\Delta K_{eff}}{\Delta K} = \frac{K_{max} - K_{op}}{K_{max} - K_{min}} = \frac{P_{max} - P_{op}}{P_{max} - P_{min}} = \frac{1 - \dfrac{P_{op}}{P_{max}}}{1 - R}$$

K_{op} is open stress intensity factor; P_{op} is crack opening loads; P_{max} is the maximum crack opening loads; P_{min} is the minimum crack opening loads

The Paris formula is:

$$\frac{da}{dN} = C \cdot \Delta K^m = C \cdot \left(\Delta K_{eff}\right)^m = C \cdot (U \cdot \Delta K)^m$$

a is the length of crack and N is cyclic times while C and m are determined by material itself

Small crack theory

Small crack theory was used to predict the fatigue lives of the shot peened and un-peened specimens.

The baseline long crack growth rates for three stress ratio of R=-1,0.06 and 0.5, and the resulting da/dN-ΔK_{eff} relationships are shown in Fig.16.

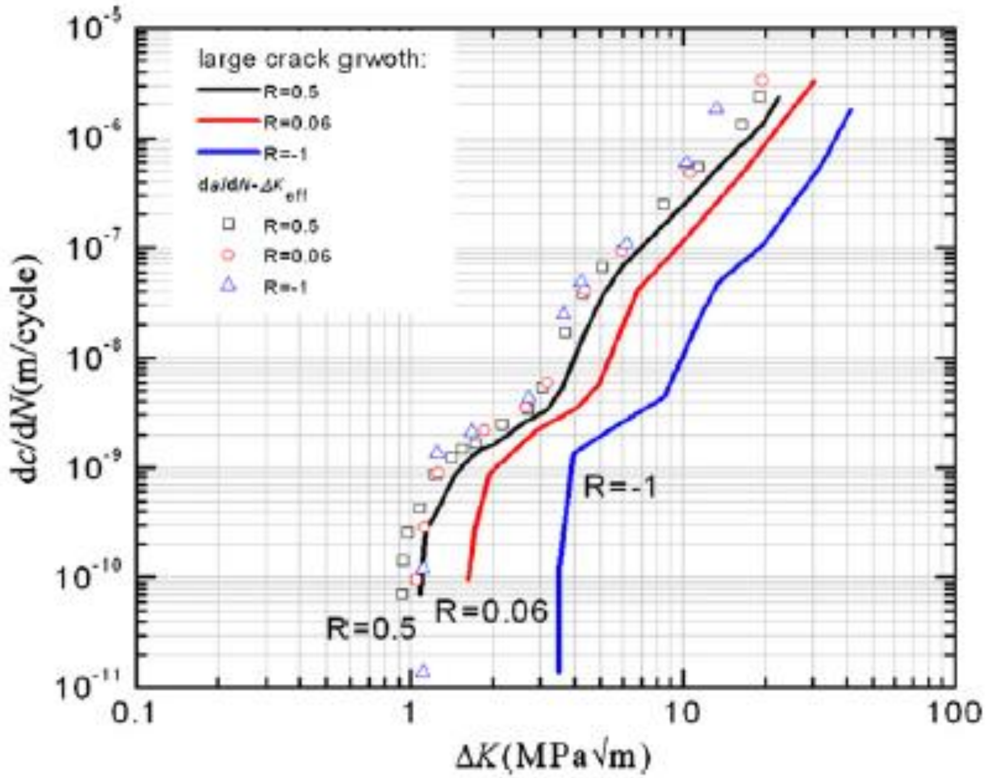

Fig.16 Baselines of long crack growth rates and closure analysis of da/dN-ΔK_{eff} in 7475-T7351 aluminum alloy.

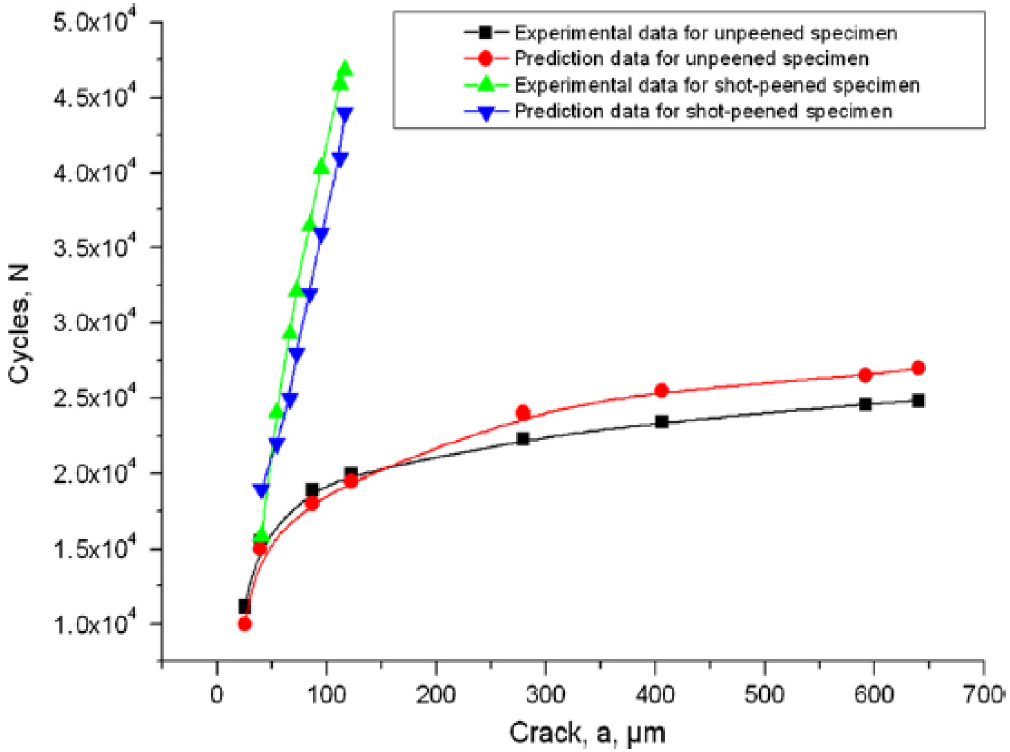

The calculated fatigue lives using Newman's FASTRAN code are in good agreement with the measured data for both the shot peened and un-peened samples (Fig.17).

Fig.17 Experimental and predicted crack length vs. cycles in 7475-T7351 alloy.

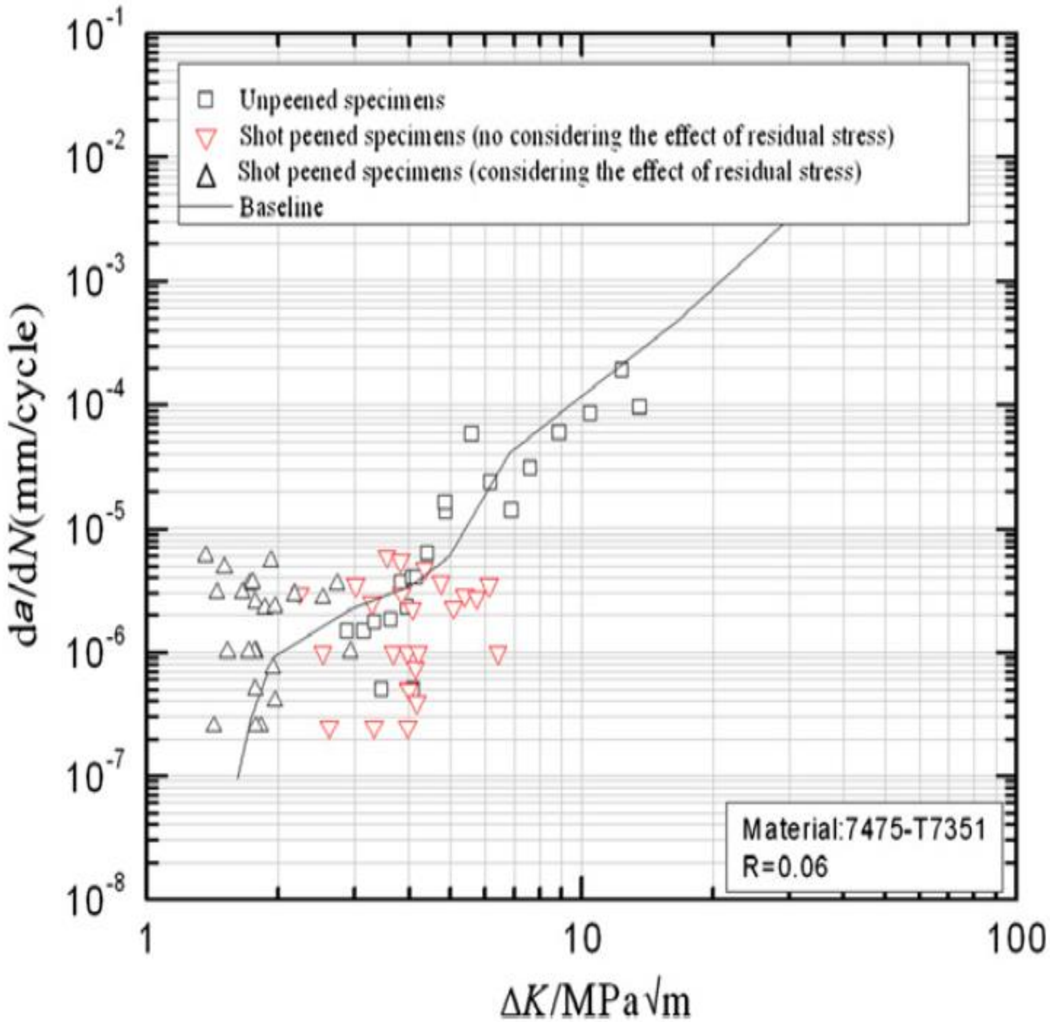

Y.K. Gao, X.R. Wu, Experimental investigation and fatigue life prediction for 7475-T7351 aluminum alloy with and without shot peeing-induced residual stresses, Acta Materialia, 59(2011):3737-3747.

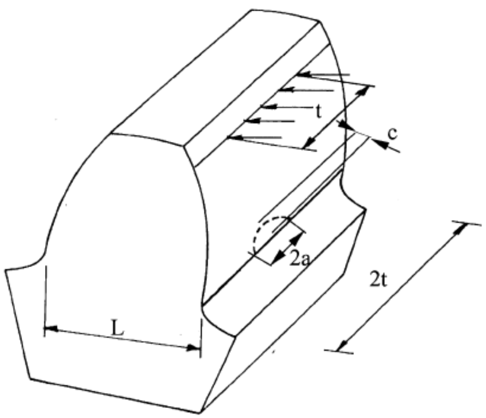
t
c
2a
2t
L

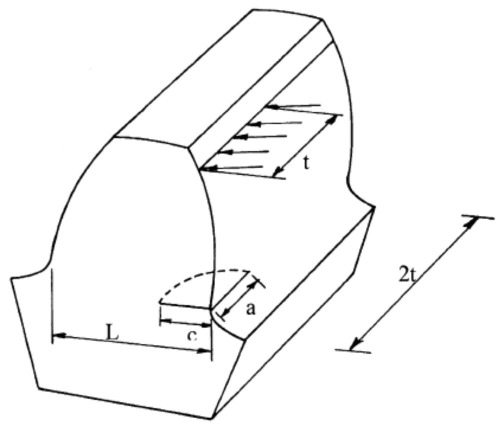
t
2t
a
L
c

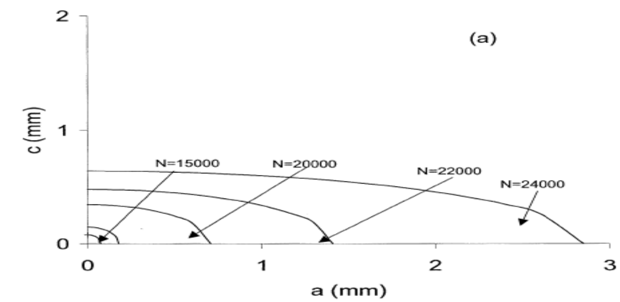
(a)
c (mm)
a (mm)
N=15000
N=20000
N=22000
N=24000
0
1
2
3

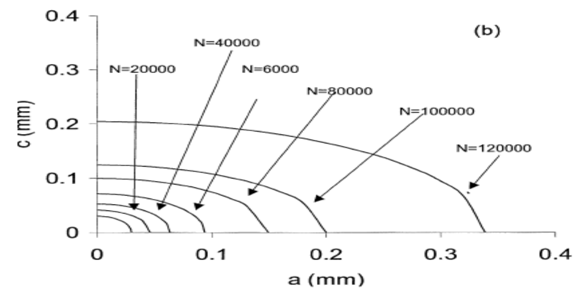
(b)
c (mm)
a (mm)
N=20000
N=40000
N=6000
N=80000
N=100000
N=120000
0
0.1
0.2
0.3
0.4

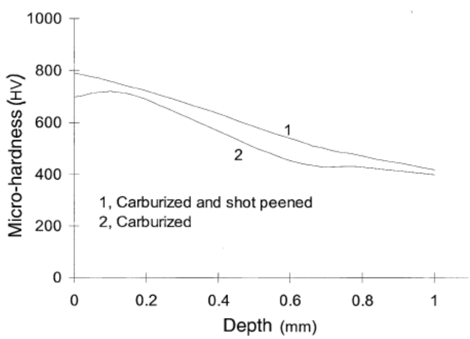
Micro-hardness (HV)
Depth (mm)
1, Carburized and shot peened
2, Carburized
1000
800
600
400
200
0
0.2
0.4
0.6
0.8
1

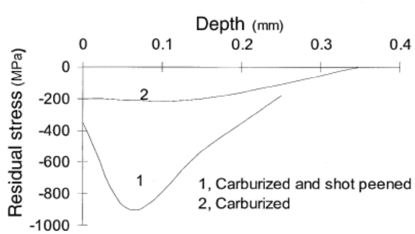
Depth (mm)
Residual stress (MPa)
1, Carburized and shot peened
2, Carburized
0
0.1
0.2
0.3
0.4
-200
-400
-600
-800
-1000

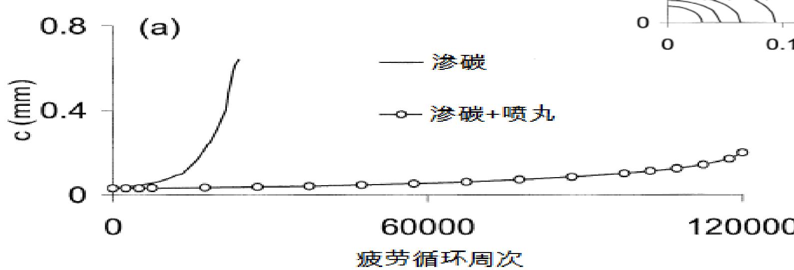
(a)
c (mm)
渗碳
渗碳+喷丸
疲劳循环周次
0.8
0.4
0
60000
120000

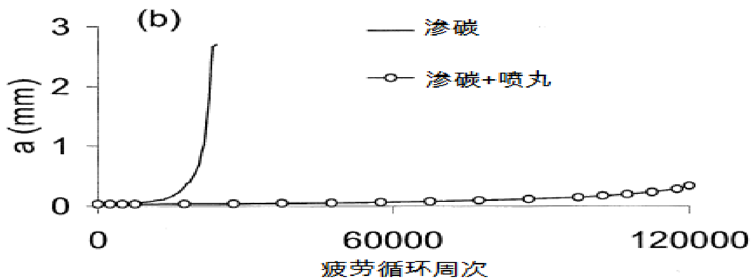
(b)
a (mm)
渗碳
渗碳+喷丸
疲劳循环周次
3
2
1
0
60000
120000

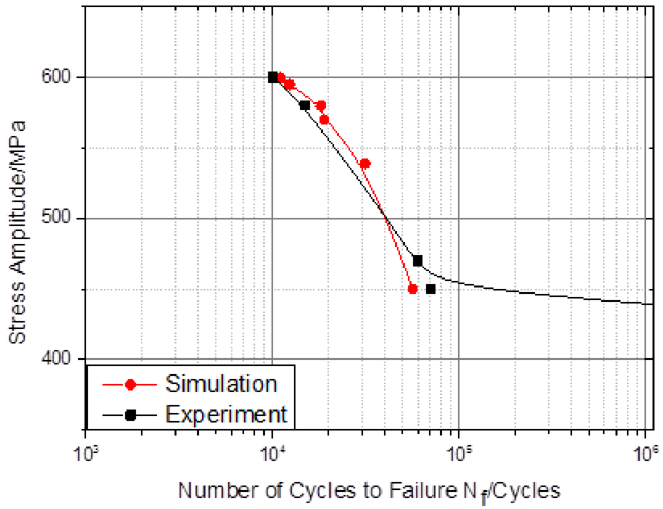

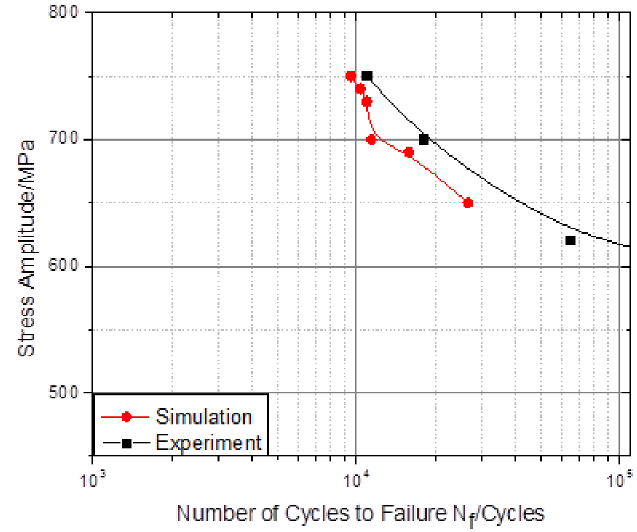

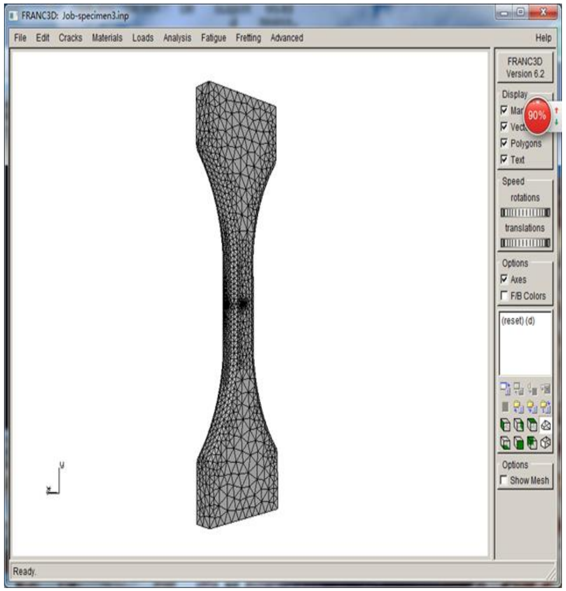

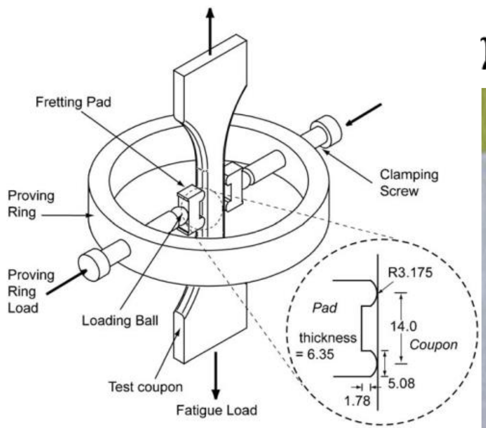

$$\gamma \times a_0 \times aN_f^b = S_{max}{}^{1} \times P$$

CuKα
λ=0.154nm
(213) 140°

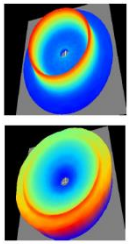

$$\gamma \times a_0 \times aN_f^b = S_{max}{}^{0.96} \times P$$

Fretting fatigue-----blade, disk, blisk, bling

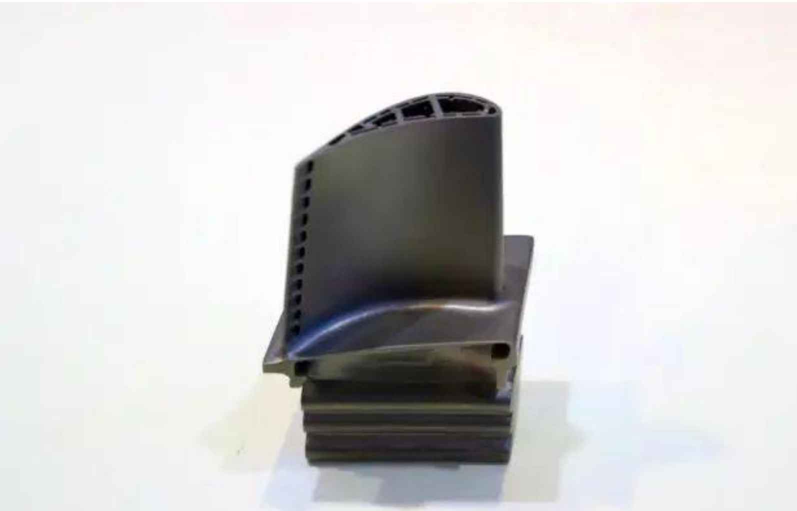

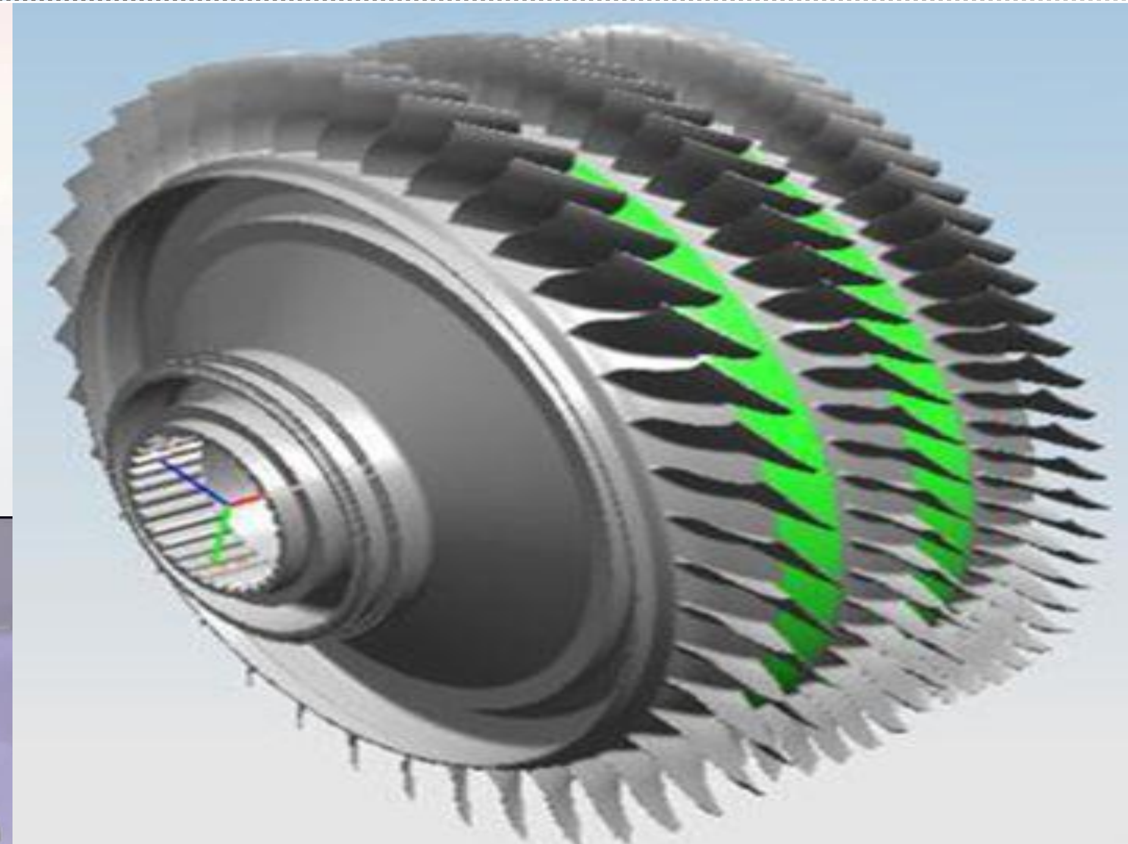

常规叶盘 整体叶盘 整体叶环

4 Conclusions and recommendations

- The fatigue sources always locate at surface for un-surface-strengthened specimens, whereas for those surface-enhanced specimens, they are located beneath the surface-enhanced layer.
- Two new concepts of surface fatigue strength/limit and internal fatigue strength/limit are proposed based on the fatigue source location and the ratio of σ_{swss} to σ_{sws} lies in the range of 1.34-1.42. This provides an easy and reasonable simply evaluation on assessing the effects of surface enhancement with sufficient accuracy.

- The electro-polishing has a beneficial effect on the fatigue limit in comparison with that of ground specimen due to the decrease of the surface toughness, but the effect is not notable. Further shot peening induces high compressive residual stress field in the surface layer, transfers the fatigue crack source into the interior and then increases the fatigue limit for about 36%.
- Shot peening greatly reduces small crack growth rates and thus significantly extends fatigue lives for materials. This beneficial effect is attributed to the compressive residual stresses induced by shot peening in the surface layer.
- By taking the residual stresses into account, total fatigue lives for materials/structures containing residual stresses can be predicted using small crack theory, by use of the crack closure-based fatigue life prediction code FASTRAN.

Acknowledgment

The author is grateful for the foundation support from National Natural Science Foundation of China (NSFC) under Grant No. 11372226 and the fundamental research Found for the Central Universities of China (FCUC) under Grant No. 13302380043.

Thanks to Professor Martin Lévesque for kind invitation to attending the ICSP13 conference in Canada.

Thanks for your attention!